International Journal of Pharmaceutics: X 3 (2021) 100068

Contents lists available at ScienceDirect

International Journal of Pharmaceutics: X

journal homepage: www.sciencedirect.com/journal/international-journal-of-pharmaceutics-x

A new engineering process of biodegradable polymeric solid implants for ultra-long-acting drug delivery

Panita Maturavongsadit [a], Gayane Paravyan [a], Martina Kovarova [c,d], J. Victor Garcia [c,d,*], S. Rahima Benhabbour [a,b,*]

[a] Joint Department of Biomedical Engineering, North Carolina State University and The University of North Carolina at Chapel Hill, Chapel Hill, NC, USA
[b] Division of Pharmacoengineering and Molecular Pharmaceutics, UNC Eshelman School of Pharmacy, University of North Carolina at Chapel Hill, Chapel Hill, NC, USA
[c] International Center for the Advancement of Translational Science, USA
[d] Division of Infectious Diseases, Center for Aids Research, School of Medicine, University of North Carolina at Chapel Hill, Chapel Hill, NC, USA

ARTICLE INFO

Keywords:
Solid implants
In-situ
Phase inversion
Compression
Long-acting drug delivery
Poly(lactic-*co*-glycolic acid)
HIV prevention

ABSTRACT

We present a long-acting (LA) biodegradable polymeric solid implant (PSI) fabricated using a new process combining in-situ phase inversion and compression. This robust process allows fabrication of solid implants that can have different shapes and sizes, accommodate high drug payloads, and provide sustained drug release over several months. Herein the integrase inhibitor dolutegravir (DTG) was used to develop PSIs for HIV prevention. PSIs were fabricated using a three-step process by (a) phase inversion of DTG-loaded polymer solution to form an initial in-situ forming implant in an aqueous solution, (b) micronization of dried DTG-loaded solid implants, and (c) compression of the micronized DTG-loaded solid implants to form the PSI. High drug loading (up to 85 wt%) was achieved in the PSIs. DTG exhibited minimum burst release in the first 24 h (<6%) and sustained release kinetics over 6 months. The release kinetics of DTG can be fine-tuned by varying drug-loading concentration, the ratio of polymer (poly(lactic-*co*-glycolic acid), PLGA) to solvent (*N*-methyl-2-pyrrolidone, NMP) and polymer (PLGA) molecular weight in the precursor solution. The physical/chemical properties of DTG were retained post-storage under accelerated storage conditions (40 °C/75% relative humidity) for 6 months. The versatility of this technology makes it an attractive drug delivery platform for HIV prevention applications.

1. Introduction

Long-acting (LA) drug delivery technologies have attracted much attention over the past decades for their application in diverse areas of medicine such as contraception (Affandi et al., 1987; Uhm et al., 2016; Mansour, 2010), anticancer therapy (Goldspiel and Kohler, 1991; Elstad and Fowers, 2009), antipsychotic treatment (Kaplan et al., 2013; Dammerman et al., 2018), ocular disease (Macoul and Pavan-Langston, 1975; Haghjou et al., 2011; Iyer et al., 2019) pain management (Barnwal et al., 2017; Nickel et al., 2012) and many other chronic diseases (Pons-Faudoa et al., 2019; Wang et al., 2020) owing to their ability to improve patient adherence and treatment outcomes. LA drug delivery technologies offer benefits over traditional systemic administration by providing sustained drug release over weeks, months or years and achieving a therapeutic effect at lower drug concentrations compared to oral dosage forms, which can eliminate the risk of unwanted side-effects (Dash and Cudworth II, 1998; Rajgor et al., 2011). Many commercial LA drug delivery technologies are in clinical use such as levonorgestrel (Norplant®, Estring®, Jadelle®) and etonogestrel (Implanon®, Nexplanon®) implants for contraception (Affandi et al., 1987; Uhm et al., 2016; Mansour, 2010), naltrexone injectables (Vivitrol®) and buprenorphine implants (Probuphine®) for treatment of opioid abuse (Barnwal et al., 2017; Kjome and Moeller, 2011). These LA drug delivery technologies are widely accepted, and over the years their use has increased substantially in many countries, including the United States (Branum and Jones, 2015; Alderks, 2013). However, there continues to be a need for LA drug delivery technologies specifically tailored to achieve optimal therapeutic doses over extended periods of time for multiple medical application, including HIV treatment and prevention for which there are a limited number of LA technologies currently available (Spreen et al., 2013; Spreen et al., 2014).

Various LA technologies are in preclinical and clinical development for HIV treatment and prevention, such as nano-based injectable formulations (Baert et al., 2009; Landovitz et al., 2016), subcutaneous

* Corresponding authors.
E-mail addresses: victor_garcia@med.unc.edu (J.V. Garcia), benhabs@email.unc.edu (S.R. Benhabbour).

https://doi.org/10.1016/j.ijpx.2020.100068

refillable nanofluidic devices (Chua et al., 2018; Pons-Faudoa et al., 2020), and topical delivery systems such as gels (Date et al., 2012; Grammen et al., 2014; García-Lerma and Heneine, 2012), vaginal films (Guthrie et al., 2018; Bunge et al., 2016) and intravaginal rings (Devlin et al., 2013; Fetherston et al., 2013; Glaubius et al., 2019). These technologies have been shown to provide sustained delivery of drug(s) over several weeks with some reaching durations of up to 4 months. Polymeric solid implants hold great promise for the development of LA drug delivery systems owing to the ability to formulate high drug payloads in a single implant, which can potentially allow for sustained-release durations that last beyond six months. Currently, the majority of available polymeric solid implants are produced using non-biodegradable polymers such as silicones, poly(urethanes), poly(acrylates) and poly (ethylene vinyl acetate) (Mansour, 2010; Barnwal et al., 2017; Shastri, 2003). As such, surgical removal of these non-biodegradable implants is required at the end of the implant treatment duration. To date, clinically used biodegradable solid implants are limited to ocular applications and are made with poly(lactic-*co*-glycolic acid) (PLGA), poly(lactic acid) (PLA), or hydroxypropyl methylcellulose (HPMC) (Haller et al., 2009; Lee and Chee, 2005). LA biodegradable solid implants being developed for HIV prevention or treatment are in the early stages of development, and a few products are investigated, including tenofovir alafenamide (TAF)-polycaprolactone (PCL) thin-film device (Schlesinger et al., 2016) and MK-8591 eluting PLA and PCL implants (Barrett et al., 2018). These solid implants are manufactured by hot-melt extrusion, solvent-casting, or compression molding, which require high temperatures and shear forces to fabricate the solid implant (Schlesinger et al., 2016; Barrett et al., 2018; Zajc et al., 2005; Dinunzio et al., 2010).

Recently, we developed an in-situ forming implant (ISFI) injectable formulations for LA delivery of dolutegravir (DTG) (Kovarova et al., 2018; Benhabbour et al., 2019). These formulations provided sustained delivery of DTG for up to 9 months and in vivo efficacy against high dose vaginal HIV challenges in a pre-clinical humanized mouse model (Kovarova et al., 2018; Benhabbour et al., 2019). In this study, adapting from the recently developed ISFIs, we developed a new and unique process to engineer polymeric solid implants (PSIs) to further improve drug loading capacity to achieve clinically translatable doses within a single administration. We report the use of phase inversion and compression techniques to fabricate a PLGA PSI that can offer high drug loading and ultra-LA release of DTG. The compression technique provides the ability to achieve high drug loadings in a small compact solid implant in addition to the ability to control the size, shape, and mechanical properties of the final PSI. The fabrication process of these PSIs involves a stepwise process of (a) phase inversion of a DTG-loaded ISFI formulation to form an initial in-situ forming solid implant in an aqueous medium, (b) micronization of dried DTG-loaded solid implants, and (c) compression of micronized DTG-PLGA solid powder (Fig. 1). Using this novel tree-step fabrication approach, the resulting PSIs are solvent-free and consist of only the polymer (PLGA) and drug (DTG) loaded at high concentrations (up to 85 wt%) to allow for translatable doses in a single compact PSI. No additional excipients were required in order to compress or stabilize the solid implant. Drug loading and release kinetics can be modulated by varying formulation composition (e.g., polymer, solvent), drug loading, implant size/shape, and the applied compression force. This new fabrication process of PLGA-based solid implants represents a promising platform for various other polymers and drugs for sustained drug delivery.

2. Materials and methods

2.1. Materials

50:50 Poly(DL-lactide-*co*-glycolide) was purchased from LACTEL (Birmingham, AL; Cat. No. B6010—1P, MW 27 kDa). *N*-methyl-2-pyrrolidone (NMP, <USP>) was received from ASHLAND (Wilmington, DE, Product Code 851263, 100% NMP). Dolutegravir (DTG) was purchased from Selleckchem (Houston, TX; S2667-DTG, S7303-RPV). Solutol-HS 15, phosphate-buffered saline (0.01 M PBS, pH 7.4), HPLC grade Acetonitrile were purchased from Sigma Aldrich (St. Louis, MO).

2.2. Preparation of ISFI formulations

In-situ forming implant (ISFI) formulations were prepared using a previously described procedure (Benhabbour et al., 2019). Briefly, a placebo formulation was prepared by adding PLGA (50:50, 27 kDa) to NMP at various weight ratios and allowing PLGA to dissolve in NMP by continuous mixing at room temperature. Next, dolutegravir (DTG) was added to the PLGA/NMP placebo solution and allowed to stir at 37 °C overnight to completely dissolve DTG and form a homogenous formulation.

To investigate the effect of PLGA/NMP weight ratio on percent drug loading capacity in ISFIs, placebo formulations were prepared with 1:2, 1:4, 1:6, 1:8 and 1:10 *w*/w ratios of PLGA/NMP. DTG was added to each placebo solution at a near saturation concentration in the formulation (110, 170, 200, 220 and 250 mg/g DTG, respectively). To further enhance the solubility of DTG in the formulation, dimethyl sulfoxide

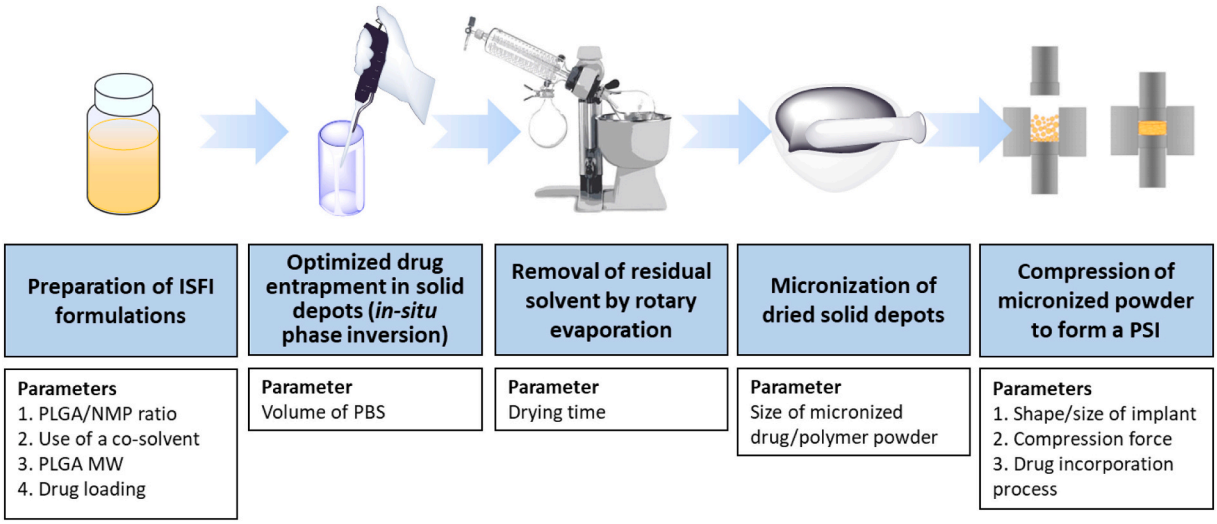

Fig. 1. Schematic illustration of the optimized fabrication process of polymeric solid implants (PSIs) and parameters that can be used to modulate drug loading capacity and drug release kinetics in the PSIs.

(DMSO) and Gelucire 44/14 were used as co-solvents with NMP at 9:1 *w*/w NMP/DMSO and 9:1 w/w NMP/Gelucire 44/14 respectively. Formulations containing co-solvents were prepared by mixing the co-solvent solution with PLGA at a weight ratio of 1:6 PLGA/solvent. This weight ratio was determined to provide the highest drug loading while still allowing solid implant formation upon injection into an aqueous medium.

2.3. Preparation of PSIs by phase inversion

Polymeric solid implants (PSIs) prepared by phase inversion were formed by either direct injection of an ISFI formulation into PBS, or injection of an ISFI formulation into a microdialysis membrane followed by incubation in PBS (Supplementary Fig. 1). To investigate the effect of shape and surface area of PSIs on drug release kinetics, three shapes of PSIs, including cube, cuboid and sphere were prepared using a 1:2 *w*/w PLGA:NMP ISFI formulation and a constant drug concentration (100 mg/g DTG). Briefly, to form a cubic and cuboid PSI, the ISFI solution (30 μL, 30 ± 2.5 mg) was injected into a microdialysis membrane with a molecular weight cut-off (MWCO) of 10 kDa (Supplementary Fig. 1A, C, D). The dialysis membranes were subsequently incubated in PBS at 37 °C for 24 h which was determined to be the optimum time to allow diffusion of NMP and formation of stable solid PSIs within the dialysis membranes. To form a spherical PSI, the ISFI solution (30 μL, 29 ± 0.5 mg) was injected directly into PBS and incubated for 24 h at 37 °C (Supplementary Fig. 1B). The PSIs were then collected and dried using a rotary evaporator for 1 h to remove all residual water prior to investigating implant microstructure and drug release kinetics. It was determined that drying times longer than 1 h did not result in change in PSI mass. Spherical PSIs were used to optimize drug loading in the final PSI and investigate the effects of PLGA/NMP ratio (1:2, 1:4, 1:6, 1:8 and 1:10 *w*/w ratios of PLGA/NMP) on implant formation, drug entrapment efficiency, implant microstructure and drug release kinetics.

To further investigate the effect of co-solvent (1:6 w/w PLGA:NMP, 1:6 w/w PLGA: (NMP/DMSO, 9:1 *w*/w), and 1:6 w/w PLGA: (NMP/Gelucire 44/14, 9:1 w/w)) on drug entrapment efficiency and drug release kinetics, PSIs were formed via phase inversion upon injection of an ISFI formulation (25 μL, 20 ± 3 mg) into PBS (2 mL) at 37 °C. After a 24 h incubation at 37 °C, PSIs were collected and dried using a rotary evaporator and tested for in vitro drug release kinetics.

2.4. Preparation of PSIs by a combination of phase inversion and compression

2.4.1. General procedure for fabrication of PSIs

To fabricate a small compact PSI with high drug payloads, a three-step fabrication process was developed using a combination of phase inversion and compression (Fig. 1). First, DTG-loaded solid implants were formed in-situ by phase inversion upon injection of the formulation solution in PBS at an optimized ratio of ISFI/PBS (25 μL:2 mL). After incubation in PBS at 37 °C for 24 h, the solid implants were collected and dried using a rotary evaporator for 1 h to remove all residual water. Dried implants were subsequently micronized using a mortar and pestle to obtain a fine powder of DTG and PLGA as a homogenous mix. To ensure uniformity and homogeneity of DTG distribution within the micronized DTG-PLGA powder, samples (1–2 mg, $n = 4$) were collected from four different areas in the solid mix and dissolved in acetonitrile, and drug concentration was quantified by HPLC analysis. The micronized DTG-PLGA powder was considered homogenous when the standard deviation of the average concentration in all 4 samples analyzed was ≤5%. The micronized DTG-PLGA powder was subsequently compressed using a single punch press tablet machine (Carver Hand Press model 3851). Briefly, 20 mg of micronized DTG-PLGA powder was loaded into a 5 mm diameter cylindrical tool and pressed at 1.274 US.ton/cm^2 for 10 s at room temperature. The final tablet formed contained PLGA and DTG with no additional additives or stabilizers.

2.4.2. Effect of PLGA MW

To assess the effects of PLGA molecular weight (MW) on drug release kinetics, PSIs were fabricated using different MWs of PLGA (11, 27 and 54 kDa). A placebo formulation was prepared with 1:6 *w*/w PLGA/solvent using a co-solvent solution of 9:1 w/w NMP/DMSO. DTG was added to the placebo solution at a near saturation concentration of 250 mg/g and allowed to stir at 37 °C overnight to fully dissolve the drug. The initial drug-loaded solid implants were formed, dried, micronized, and the resulting powder was compressed into 5-mm diameter PSIs using the aforementioned procedure. The resulting PSIs were tested to assess the effect of PLGA MW on the in vitro release kinetics of DTG.

2.4.3. Effect of drug loading

To assess the effect of DTG loading on drug release kinetics, PSIs were fabricated with five different concentrations of DTG. A placebo formulation was prepared with 1:6 *w*/w PLGA/solvent using a co-solvent solution of 9:1 w/w NMP/DMSO. DTG was added to the placebo solution at a concentration of 62.5, 125, 250, 300 and 600 mg/g and allowed to stir at 37 °C overnight to fully dissolve the drug. The initial drug-loaded solid implants were formed, dried, micronized, and compressed into 5-mm diameter PSIs using the procedure described above. The resulting PSIs containing different percent DTG loading (22.5, 45, 55, 65 and 85 wt%) were evaluated to determine the effect of DTG loading in a PSI on the in vitro release kinetics.

2.4.4. Effect of compression force

To assess the effect of compression force used in the fabrication process on the mechanical properties and microstructure of the resulting PSIs and drug release kinetics, PSIs were fabricated using three different compression forces. First, a placebo formulation was prepared with 1:6 *w*/w PLGA/solvent using a co-solvent solution of 9:1 w/w NMP/DMSO. DTG was added to the placebo solution at a near saturation concentration of 250 mg/g and allowed to stir at 37 °C overnight to fully dissolve the drug. The initial drug-loaded solid implants were formed by phase inversion, dried, and micronized using the aforementioned procedure. The micronized homogenous DTG-PLGA power (75 mg) was loaded into a 10-mm cylindrical tool and compressed at different compression forces of 0.5, 1, and 1.5 US.ton (equivalent to 0.657, 1.274, 1.911 US.ton/cm^2, respectively) to produce the final PSIs. The resulting 10-mm diameter PSIs were evaluated to compare their mechanical properties, microstructure and DTG release kinetics in vitro.

2.4.5. Effect of drug incorporation process

DTG was formulated in the PSIs using either a pre-loading process whereby DTG was added in the placebo solution formulation, as described above, or using a post-loading process whereby DTG was added to a preformed micronized polymer powder. The effect of DTG loading process on in vitro drug release kinetics was investigated. In the pre-loading process, DTG was added to a placebo solution (1:6 *w*/w PLGA/(NMP/DMSO, 9:1 *w*/w)) at a near saturation concentration of 250 mg/g, and 5-mm diameter PSI (60% w/w DTG) was fabricated using the aforementioned procedure. In the post-loading process, a micronized PLGA powder was first prepared by generating solid implants via in-situ phase inversion of a 1:6 w/w PLGA/(NMP/DMSO, 9:1 *w*/w) placebo solution precursor. The solid implants were subsequently dried and micronized as described above. DTG was added to the pre-formed micronized PLGA powder to achieve the same concentration of DTG (60% *w*/w) obtained in the pre-loaded PSIs, and the drug/polymer solid mix was used to produce a 5-mm diameter PSI.

2.5. Drug loading capacity

To optimize percent drug loading within PSIs, the saturation concentrations of DTG in ISFI formulations containing 1:2, 1:4, 1:6, 1:8 and 1:10 *w*/w PLGA:NMP, as well as 1:6 w/w PLGA: (9:1 NMP/co-solvent), were determined. DTG (30 mg) was added to individual vials containing

100 mg of PLGA:NMP or PLGA/(NMP:DMSO 9:1). The solution was mixed thoroughly using a combination of vortex mixing and short heating cycles (~40 °C) for a few minutes (3–5 min), and was stirred for an additional 24 h at 37 °C to allow DTG to fully dissolve in the formulation. Samples were subsequently centrifuged for 30 min at 13,000 rpm (Eppendorf Centrifuge 5417C, USA) to remove the excess undissolved drug. Sample aliquots (1 mg, $n = 4$) were collected from the drug saturated supernatant and dissolved in acetonitrile (ACN) to quantify DTG concentration by HPLC analysis.

Reverse-phase HPLC analyses were carried out with a Finnigan Surveyor HPLC system (Thermo Finnigan, San Jose, California, USA) equipped with a Photodiode Array (PDA) Plus Detector, auto-sampler, and LC Pump Plus. The stationary phase utilized for the analysis was an Inertsil ODS-3 column (4 μm, 4.6 Å ~ 150 mm, [GL Sciences, Torrance, CA]) maintained at 40 °C. Chromatographic separation was achieved by gradient elution using a mobile phase consisting of 0.1% trifluoroacetic acid in water and ACN (H_2O/ACN 95:5 *v*/v). The flow rate was 1.0 mL/min and the total run time was 25 min for each 25 μL injection.

2.6. Drug entrapment efficiency

Drug entrapment efficiency was determined as the maximum drug entrapped in solid implants formed in the initial step of PSI fabrication by phase inversion. The entrapment efficiency was used to assess formulation parameters that result in optimized drug loading in the final PSI. DTG ISFI formulations were prepared with 1:2, 1:4, 1:6 1:8 and 1:10 *w*/w PLGA/NMP, as well as 1:6 w/w PLGA/(NMP/co-solvent, 9:1 *w*/w) and near saturation concentrations of DTG (C_{loaded}) in each formulation (110 mg/g, 170 mg/g, 200 mg/g, 220 mg/g, 260 mg/g, 250 mg/g (co-solvent, DMSO) and 230 mg/g (co-solvent, Gelucire44/14) respectively). Sample aliquots (20–25 μL) from each ISFI formulation were injected into 2 mL PBS and incubated at 37 °C for 24 h to quantify percent DTG entrapment in the solid implants. Sample aliquots (1 mL) from the release medium were collected 24 h post-incubation and DTG concentration was quantified by HPLC analysis to determine the 'free' drug released during the phase inversion step (C_{free}) in the process of solid implant formation. Percent DTG entrapment in the solid implants was calculated using the equation below. All experiments were performed in quadruplicate.

$$\%DTG\ entrapment = \frac{\text{Cloaded} - \text{Cfree}}{\text{Cloaded}} \times 100$$

2.7. Scanning electron microscopy (SEM) imaging

To investigate drug distribution and microstructure of DTG PSIs prepared by phase inversion, PSIs were prepared with varying *w*/w ratios of PLGA/NMP (1:2, 1:4, 1:6 and 1:8 w/w PLGA/NMP) and varying concentration of DTG (100 and 110 mg/g, 170 mg/g, 200 mg/g and 220 mg/g respectively). To investigate drug distribution, microstructure and physical state of drugs after the micronization step, micronized DTG-PLGA powders were prepared from 1:6 w/w PLGA/(NMP/DMSO, 9:1) (250 mg/g DTG) ISFI solutions using the method described above. The resulting DTG PSIs and micronized DTG-PLGA powders were mounted on an aluminum stub using carbon tape, and sputter coated with 5 nm of gold-palladium alloy (60:40) (Hummer X Sputter Coater, Anatech USA, Union City, CA). The coated samples were imaged using a scanning electron microscope with an acceleration voltage of 5 kV, 30 μm aperture, and average working distance of 15 mm (Zeiss Supra 25, Carl Zeiss Microscopy, LLC, Thornwood, NY). SEM imaging analysis was also carried out to investigate the effect of compression force on the microstructure of PSIs. PSIs generated with varying compression forces using 1:6 *w*/w PLGA/(NMP/DMSO, 9:1) formulation with the methods described above were flash-frozen in liquid nitrogen and lyophilized for 24 h prior to SEM imaging analysis.

2.8. Thermogravimetric analysis

To assess the physical state of DTG and PLGA in PSIs, differential scanning calorimetry (DSC) analyses of pure drug (DTG), optimized placebo PSIs, and optimized DTG PSIs were carried out using a differential scanning calorimeter (TA Q200, USA). Prior to DSC analysis, decomposition temperature (T_d) of DTG was determined using a thermogravimetric analyzer (TGA, TA Q500, USA). Briefly, pure DTG was weighed (10 mg), sealed in an aluminum pan, and placed into a thermogravimetric analyzer. The DTG sample was heated from 0 to 600 °C at a ramp-up rate of 10 °C/min under inert nitrogen gas introduced at a flow rate of 20 mL/min.

For DSC analysis, samples (3–5 mg DTG, 5–10 mg DTG or placebo PSIs) were weighed, hermetically sealed in an aluminum pan and subsequently placed in a differential scanning calorimeter. For each measurement, samples were heated from 0 to 250 °C at a rate of 10 °C/min under nitrogen (20 mL/min flow rate). The DSC thermograms were used to determine the peak glass transition temperature (T_g) of PLGA, melting point (T_m) of DTG, and the physical state of DTG in PSIs (i.e. crystalline or amorphous).

2.9. Mechanical properties of PSIs

To evaluate the mechanical properties of PSIs prepared with varying compression forces, a three-point bending test was performed on a RSAIII micro-strain analyzer (TA Instruments, USA) fitted with three-point bending geometries. For each measurement, a 10-mm diameter PSI tablet was placed on the lower 3-point bending tool, and the sample was then tested with a 35 N load cell at a strain rate of 0.05 mm/s until a fracture was observed within the tablet.

2.10. In vitro release studies

To investigate the ability to fine-tune drug loading, drug release kinetics, and achieve ultra-long-acting drug release (>3 months) using PSIs, in vitro release studies were carried out with various DTG PSIs prepared by phase inversion only or by a combination of phase inversion and compression. For the DTG PSIs prepared by phase inversion only, DTG release kinetics were assessed by incubating DTG PSIs into 200 mL of release medium (0.01 M PBS with 2% Solutol HS, pH 7.4) under sink conditions at 37 °C for up to 6 months. Sink conditions were defined as DTG concentration at or below 1/5 of its maximum solubility (i.e. ≤ 0.12 mg/mL DTG) in PBS/Solutol at 37 °C. Sample aliquots (1 mL) were collected at various time points and replaced with fresh release medium. The release medium was completely removed and replaced with fresh medium every week to maintain sink conditions. DTG concentration in release samples was quantified by HPLC analysis. Cumulative drug release was normalized to the total concentration of drug in the implant determined by HPLC analysis. All experiments were performed in quadruplicates. For DTG PSIs prepared by the combination of phase inversion and compression, DTG release kinetics were assessed by incubating 5-mm or 10-mm diameter DTG PSIs (20 mg ± 0.2 mg or 75 mg ± 0.5 mg respectively) in 200 or 500 mL of release medium (0.01 M PBS pH 7.4 with 2% Solutol HS) at 37 °C for up to 6 months under sink conditions. Sample aliquots (1 mL) were collected, and DTG concentration was quantified by HPLC analysis. All experiments were performed in triplicates.

2.11. Accelerated stability studies

DTG PSIs (65 wt% DTG) were selected based on their optimal DTG release kinetics to assess their long-term stability under accelerated storage conditions. The DTG PSIs were stored in a desiccator for 6 months at 40 °C/75% relative humidity (RH) in a Fisher Scientific Isotemp Incubator (Pittsburgh, PA). PSIs ($n = 3$) were collected at various time intervals (0, 14 days, 1, 3, and 6 months) and analyzed by HPLC for

drug content and presence of any degradation products. Zero-time samples were used as controls (i.e. 100% DTG concentration).

2.12. In vitro HIV-1 inhibition

TZM-bl cells (NIH AIDS Research and Reference Reagent Program, catalog number 8129, passage number 2–6) were cultured in TZM-bl medium containing Dulbecco's Modified Eagle Medium (Sigma) supplemented with 10% fetal bovine serum, 25 mM HEPES, 500 units/ml penicillin, 50 μg/ml streptomycin and 2 mM L-glutamine (Cellgro) at 37 °C, 10% CO_2. For HIV-1 inhibition assay, TZM-bl cells at a density of 1×10^5 cells per well in TZM-bl medium were plated in 96-well plates. After 24 h of incubation, the medium was removed, replaced with 100 μl of 1:100 dilutions of DTG, and incubated for 30 min at 37 °C, 10% CO_2. Cells were subsequently infected with HIV-$1_{JR\text{-}CSF}$ by adding 100 μl of TZM-bl medium containing 40 μg/ml of DEAE-dextran and 3×10^3 TCIU of HIV-$1_{JR\text{-}CSF}$ per well. After 48 h of incubation, luciferase activity of TZM-bl cells infected with HIV-1 was quantified using One-Glo luciferase assay. Briefly, the medium was removed and the luciferase substrate One-Glo reagent (Promega, Madison, WI) supplemented with 0.2%Triton X-100 was added to allow for the measurement of luciferase activity and to inactivate virus. Luciferase was measured with a SpectraMax M3 Spectrometer (Molecular Devices, Sunnyvale, CA) and the results normalized to the luciferase activity of cells infected with HIV in the absence of DTG and expressed as a percentage of decrease in luciferase activity. Luciferase activity was measured in 3 independent experiments, each dilution measured in quadruplets. The effective drug concentrations required to inhibit virus replication by 50% (IC50) was calculated by fitting data to a sigmoid dose-response curve with a variable slope using GraphPad Prism.

2.13. Preparation of HIV-$1_{JR\text{-}CSF}$ stocks for infection

293 T cells were cultured at 37 °C, 10% CO_2 in Dulbecco's Modified Eagle Medium supplemented with 10% fetal bovine serum, 25 mM HEPES, 500 units/ml penicillin, 50 μg/ml streptomycin and 2 mM L-glutamine. Cells were regularly checked for morphology by microscope. Viral stock of HIV-$1_{JR\text{-}CSF}$ was generated by transfecting proviral DNA (Keele et al., 2008; Koyanagi et al., 1987; Ochsenbauer et al., 2012; Permar et al., 2013; Salazar-Gonzalez et al., 2009) into 293 T cells (American Tissue Culture Collection, catalog number CRL-3216, passage <10) using Lipofectamine 2000 (Invitrogen). Viral particles were collected from the tissue culture medium, pre-cleared by centrifugation (3000 RPM for 20 min at 4 °C). Tissue culture infectious units (TCID)/ml of HIV was determined by titration on TZM-bl cells. The infected TZM-bl cells were visualized with staining solution (4 μM potassium ferrocyanide, 4 μM potassium ferricyanide, 2 μM magnesium chloride, 0.4 mg/ml X-gal) (Kovarova et al., 2015; Wahl et al., 2012).

2.14. Statistical analysis

Data were represented as means ± standard deviation (SD) and analyzed with GraphPad Prism (version 6.01) via the one-way analysis of variance (ANOVA). The confidence levels were set as 95% ($p^* < 0.05$) and 99% ($p^{**} < 0.01$).

3. Results

3.1. Characterization of PSIs prepared by phase inversion

3.1.1. Effect of implant shape and surface area on DTG release kinetics

Surface area of solid implants can influence the in vitro and in vivo release kinetics of drugs from the implants (Goyanes et al., 2015). This study aimed to investigate if the surface area of PSI impacts the release kinetics of DTG. We used the PSI fabricated by phase inversion of ISFI as a prototype to understand this impact. Herein, three implant shapes (cuboid, cube, and sphere) were prepared to investigate the effect of implant surface area on drug release kinetics. The specific surface areas (SSA, SA/V) determined for the cuboid, cubic, and spherical PSIs were 3.99, 2.49 and 0.74 mm^3/mg, respectively (Fig. 2A). PSIs with higher SSA (cuboid and cube) showed higher burst after 24 h (20% cuboid and 18% cube, $p < 0.01$) and faster release kinetics of DTG ($p < 0.0001$) compared to significantly lower burst (2%) and slower release kinetics obtained with spherical implants (Fig. 2B). At later time points (>49 days), the swelling properties of PSIs had a significant impact on the release kinetics of DTG. After ~35 days incubation in PBS at 37 °C, the cuboid and cube implants had a significant increase (20% d35-d63, $p < 0.05$) in percent DTG release due to swelling (Fig. 2C). The spherical implants showed a significant increase (75% d49-d105, $p < 0.0001$) in DTG percent release after ~9 weeks of incubation in PBS at 37 °C (Fig. 2B, C). SEM imaging analyses of DTG PSIs post-incubation for 8, 12, and 16 weeks were carried out as a corroborative method to investigate the effect of PSI microstructure on drug release from PSIs overtime. The images showed a depleted amount of DTG overtime in each PSI shape (Fig. 2D). At 8 weeks, PSIs with higher SSA (cuboid and cube) showed less DTG content compared to the spherical PSIs. No DTG was detected in the cuboid and cubic PSIs after 12 and 16 weeks indicating the completion of drug release, which was in agreement with the release data determined by HPLC analysis (Fig. 2B).

3.1.2. Effect of PLGA:NMP weight ratio on drug loading and release kinetics

High drug loading in the initial ISFI formulation combined with high percent drug entrapment during the phase inversion step results in high drug loading in the final PSI. Results showed that DTG concentration in the initial ISFI formulations increased with increasing solvent ratio and was highest in 1:10 *w*/w PLGA:NMP (~280 mg/mL). The lowest DTG concentration (~124 mg/mL) was obtained with the 1:2 w/w PLGA/NMP ISFI formulation (Fig. 3A).

The formation of initial solid implants by in-situ phase inversion is a required and important step to successfully generate PSIs with high percent drug loading. Solid implants were successfully formed as stable spheres with ISFI formulations containing 1:2, 1:4, 1:6 and 1:8 *w*/w PLGA:NMP after incubation in PBS for 24 h at 37 °C. With higher solvent content (1:10 w/w PLGA/NMP) solid spherical implants were not able to form upon injection of the ISFI formulation in PBS and incubation for 24 h at 37 °C (Fig. 3B).

Drug entrapment efficiency was determined with ISFI formulations that resulted in stable spherical solid implants (1:2, 1:4, 1:6, and 1:8 w/w PLGA:NMP) to determine the maximum DTG concentration that can be formulated in a PSI. The percent DTG entrapment in solid implants was determined by quantifying DTG released into PBS during the phase inversion step. For the four ISFI formulations tested, DTG percent entrapment was ≥90% and increased with increasing the amount of NMP in the formulation (Fig. 3A).

The drug distribution and microstructure of solid implants can influence drug release kinetics in vitro and in vivo (Benhabbour et al., 2019; Fu and Kao, 2010). SEM imaging analysis of spherical DTG PSIs showed that DTG exhibited a different distribution in PSIs generated from ISFI formulations containing different ratios of PLGA:NMP (Fig. 3C). ISFI formulations containing the lowest amount of NMP (1:2 *w*/w PLGA/NMP) resulted in PSIs with DTG uniformly distributed throughout the dense polymer matrix implant (Fig. 3C). On the other hand, ISFI formulations containing higher amounts of NMP (1:4, 1:6 and 1:8 *w*/w PLGA:NMP) resulted in PSIs with DTG mainly distributed within the core of the implant, which can potentially be attributed to a faster phase inversion with higher amounts of NMP in the formulation (Fig. 3C).

To further investigate the effect of drug distribution in spherical PSIs and their microstructure on drug release kinetics, in vitro release studies were carried out over six months. Results shown in Fig. 3 demonstrate that spherical PSIs generated from ISFI formulations containing the

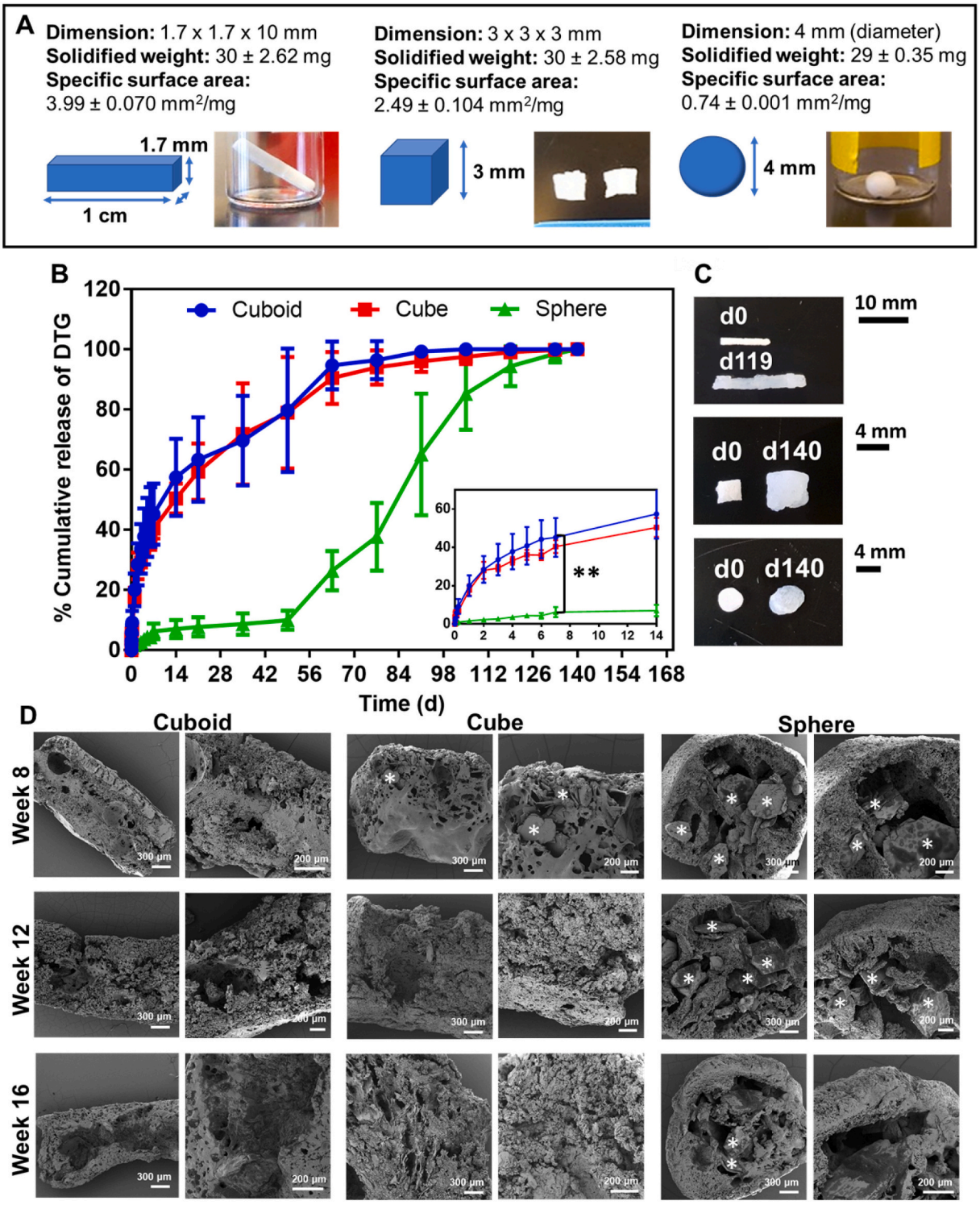

Fig. 2. Effect of implant surface area on drug release kinetics. A) Implant dimensions, weight, and specific surface area for three different shapes (cuboid, cube, and sphere). The specific surface area was quantified using PSI weight and dimensions (mm^2/mg, $n = 4$); B) In vitro release kinetics of DTG from PSIs with different shapes incubated at 37 °C for 140 days. All implants (~30 g, $n = 4$) contained ~10 wt% DTG. Graph inset represents the release kinetics of DTG during the initial 2 weeks; C) Images of the DTG PSIs before and after completion the release studies. An increase in the specific surface area was observed for all implant shapes; D) SEM images representing cross-section images of the DTG PSIs with various shapes post-incubation in PBS at 37 °C for 8, 12, and 16 weeks. The white * symbols represent DTG in the DTG PSIs.

lowest amount of NMP (1:2 *w*/w PLGA/NMP) resulted in the lowest DTG loading (20 wt% DTG) and exhibited the slowest release kinetics (~5% at week 4). On the other hand, spherical PSIs generated from ISFI formulations with the highest NMP content (1:8 w/w PLGA/NMP) resulted in the highest DTG/PLGA loading (65 wt% DTG) and exhibited the fastest release kinetics (100% by week 4, Fig. 3D). The average DTG release rate within the first 42 days was calculated using the slopes of the linear equations generated from data points within the first 42 days and

A

ISFI formulation	DTG loading capacity in ISFI		DTG entrapment in PSI (%)	PLGA/DTG in PSI (% w/w)	DTG burst at 24h (%)	DTG burst at 24h (μg)	DTG release rate at zero order kinetics (μg/day)
	w/w (mg/g)	w/v (mg/mL)					
1:2 PLGA:NMP	112.94 ± 2.97	124.24 ± 3.26	89.87 ± 1.58	79.64 ± 0.29	1.88 ± 0.16	37.35 ± 3.10	0.80 (R^2 = 0.9910)
1:4 PLGA:NMP	174.83 ± 4.16	192.32 ± 4.57	91.51 ± 1.13	59.34 ± 0.30	4.98 ± 0.70	188.14 ± 35.08	12.72 (R^2 = 0.9856)
1:6 PLGA:NMP	210.81 ± 2.90	231.89 ± 3.19	92.31 ± 0.50	45.65 ± 0.13	8.46 ± 2.02	378.57 ± 92.48	55.34 (R^2 = 0.9734)
1:8 PLGA:NMP	217.87 ± 6.22	239.66 ± 6.84	95.96 ± 0.28	34.70 ± 0.07	18.46 ± 6.07	1054.94 ± 345.96	309.76 (R^2 = 0.9506)
1:10 PLGA:NMP	256.81 ± 9.80	282.48 ± 10.78	N/A	N/A	N/A	N/A	N/A

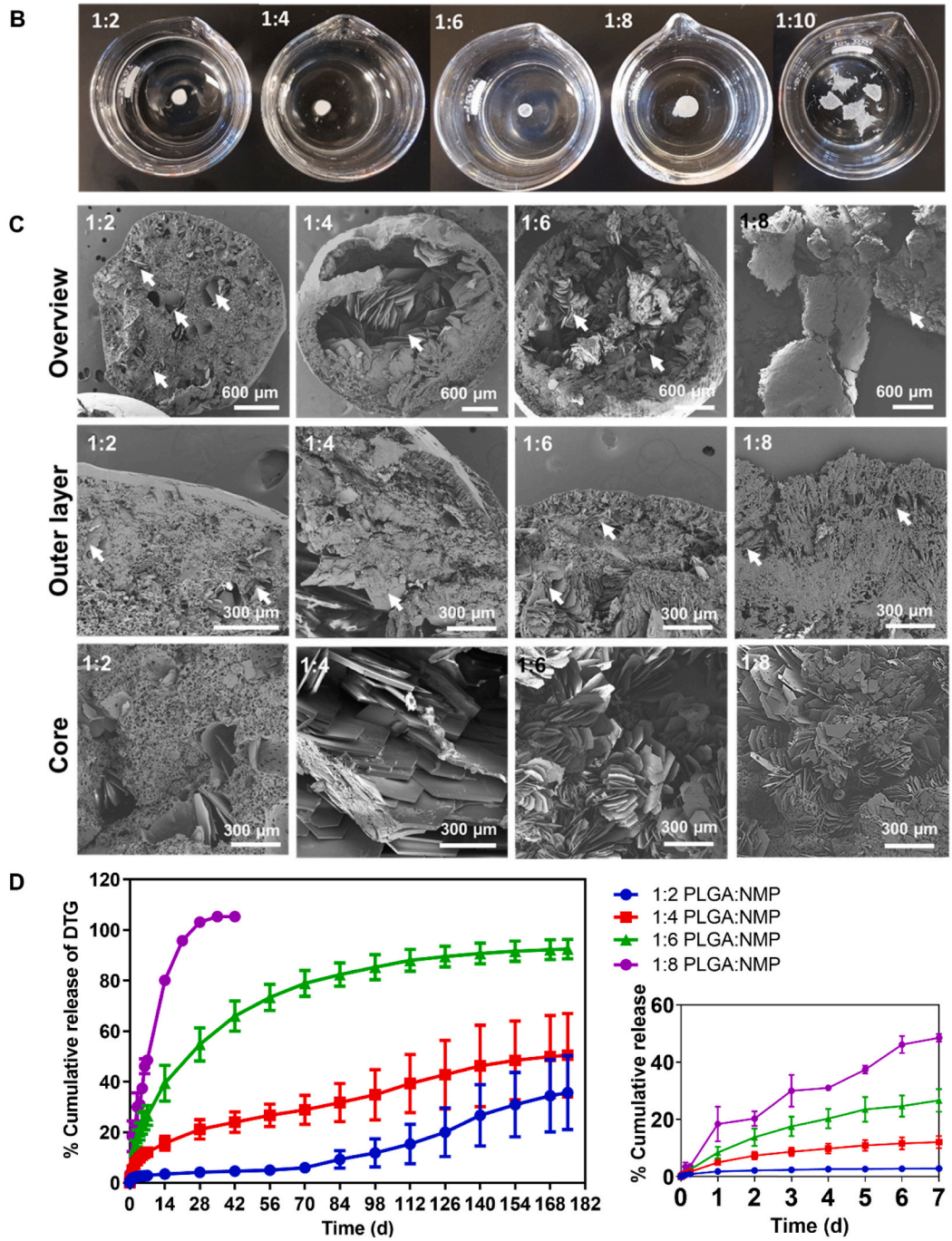

Fig. 3. Effect of PLGA:NMP weight ratio in initial ISFI formulations (1:2, 1:4, 1:6, 1:8, and 1:10 w/w PLGA/NMP) on: A) Loading and percent entrapment of DTG in PSIs, and in vitro release kinetics of DTG at 37 °C for 180 days ($n = 4$). B) Structures of PSIs formed by direct injection of ISFI solutions (n = 4) in PBS at 37 °C. C) SEM images representing cross-sections of DTG PSIs generated from initial ISFI formulations containing various PLGA/NMP ratios (1:2, 1:4, 1:6 and 1:8 *w*/w PLGA/NMP). D) In vitro release kinetics of DTG PSIs containing varying DTG:PLGA ratios (20%, 40%, 55% and 65% w/w DTG/PLGA prepared from the 1:2, 1:4, 1:6 and 1:8 w/w PLGA/NMP ISFIs, respectively). Inset represents the release kinetics within the first 7 days. All error bars represent standard deviation for $n = 4$.

estimated at 0.80, 12.72, 55.34, and 309.76 μg/day for the PSIs prepared using 1:2, 1:4, 1:6, and 1:8 *w*/w ratio PLGA:NMP formulations respectively (Fig. 3A). Drug distribution and microstructure analyses of DTG PSIs post-incubation for 4, 8, 12, and 16 weeks were used as a corroborative method to correlate the effect of DTG distribution within the PSI and DTG physical state (crystalline vs amorphous) to its in vitro release kinetics. The results demonstrated a decrease in DTG content due to release from the implant and a decrease in polymer content due to degradation over 4–16 weeks for PSIs prepared with 1:2, 1:4 and 1:6 *w*/w ratio PLGA:NMP formulations. In comparison, no DTG was present in PSIs prepared with 1:8 w/w PLGA/NMP after 4 weeks incubation (Supplementary Fig. 2, 3), which is in agreement with the release data determined by HPLC analysis (Fig. 3D). Based on the sustained release kinetics (>6 months) and release rate ~ 55 μg/day, the 1:6 *w*/w PLGA/NMP ratio was selected as the optimal formulation to generate PSIs with high drug payloads that can translate to effective concentrations (4 × PAIC90) known as a benchmark requirement to inhibit HIV infection (Adams et al., 2013; Radzio et al., 2015; Andrews et al., 2014).

3.1.3. *Effect of co-solvent on drug loading and release kinetics*

Drug solubility in an ISFI formulation can be improved using a co-solvent system. Dimethyl sulfoxide (DMSO) and Gelucire (44/14) (Gel) were investigated as co-solvents with NMP and showed a significant increase in DTG solubility compared to NMP only. With DMSO as a co-solvent (9:1 *w*/w NMP/DMSO) the solubility of DTG significantly increased from ~231.89 mg/mL (1:6 w/w PLGA:NMP) to ~276.64 mg/mL (1:6 w/w PLGA/(NMP/DMSO 9:1 *w*/w), $p < 0.0001$). With Gelucire (44/14) (Gel), the solubility of DTG increased from ~231.89 mg/mL (1:6 w/w PLGA:NMP) to ~259.59 mg/mL (1:6 w/w PLGA/ (NMP/Gel 9:1 w/w), $p = 0.0004$) (Fig. 4A). Spherical PSIs generated with ISFI formulations containing NMP only or a co-solvent system exhibited high percent entrapment of DTG (≥96%) (Fig. 4A). Based on the solubility data, DMSO was selected as a co-solvent to investigate in vitro release kinetics of DTG from PSIs with higher DTG content. As shown in Fig. 4B, C spherical PSIs generated with 1:6 *w*/w PLGA:NMP and 1:6 w/w PLGA/(NMP/DMSO 9:1) formulations resulted in 59.67 wt% and 64.14 wt% DTG respectively. Both spherical PSIs exhibited minimum initial burst release of DTG in the first 24 h (~5% DTG). The average DTG release rate within the first 42 days calculated from the zero order linear slope was ~63 and 73 μg/day with no significant difference ($p > 0.05$) for DTG PSIs prepared from the 1:6 PLGA/NMP and 1:6 PLGA/(NMP:DMSO) formulations respectively. Collectively, this data showed that using DMSO as a co-solvent significantly improved DTG loading in PSIs without altering in vitro drug release kinetics.

A

ISFI formulation	DTG loading capacity in ISFI		DTG entrapment in PSI (%)	DTG/PLGA ratio in PSI (wt%)
	w/w (mg/g)	w/v (mg/mL)		
1:6 PLGA:NMP	210.81 ± 2.90	231.89 ± 3.19	96.68 ± 0.39	59.66 ± 0.10
1:6 PLGA/(NMP/DMSO, 9:1)	251.90 ± 8.20	276.64 ± 9.02	98.19 ± 0.17	64.14 ± 0.04
1:6 PLGA/(NMP/Gelucire44/14, 9:1)	235.99 ± 5.57	259.59 ± 6.13	97.88 ± 0.18	61.74 ± 0.00

B

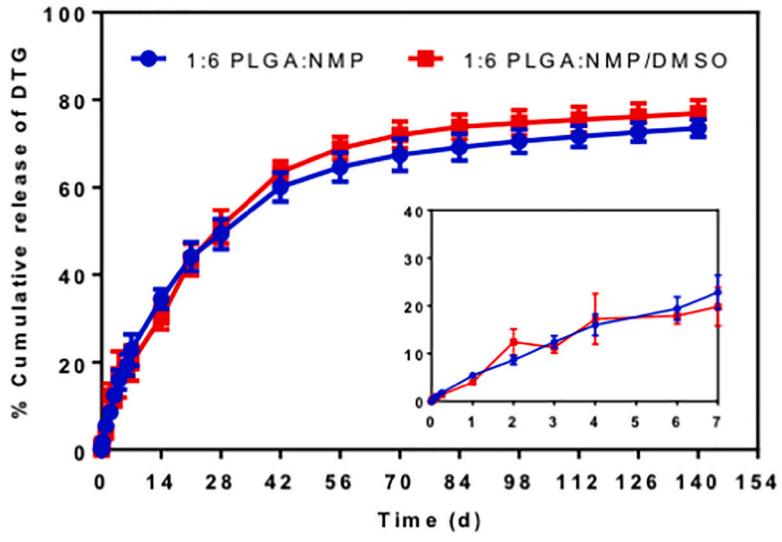

C

ISFI formulation	DTG/PLGA ratio in PSI (wt%)	DTG burst at 24 h (%)	DTG burst at 24 h (μg)	DTG release rate within days 0-42 (μg/day)
1:6 PLGA:NMP	59.66 ± 0.10	5.45 ± 0.48	332.98 ± 31.24	63.35 (R^2 = 0.9607)
1:6 PLGA/(NMP/DMSO, 9:1)	64.14 ± 0.04	4.00 ± 0.19	234.99 ± 16.57	73.83 (R^2 = 0.9723)

Fig. 4. Effect of co-solvents in ISFI formulations on drug solubility and release kinetics. A) DTG loading and percent entrapment in PSIs; B) In vitro release kinetics of DTG PSIs at 37 °C for 140 days. DTG PSIs were prepared with 1:6 *w*/w PLGA/NMP and 1:6 w/w PLGA/(NMP/DMSO, 9:1) ISFIs formulations. DTG was loaded at a near saturated concentration in each formulation (~200 mg/g and 250 mg/g respectively). Inset represents the release kinetics within the first 7 days. All error bars represent standard deviation for $n = 4$; C) Summary of release kinetics including initial burst release and zero-order release rate within the first 42 days for PSIs described in B.

3.2. Characterization of PSIs fabricated by phase inversion and direct compression

3.2.1. Physical properties of DTG PSIs

To achieve a translational dose of DTG (≥600 mg (Murray et al., 2018; Clement et al., 2020)) in a 1:6 *w*/w PLGA:(NMP/DMSO, 9:1 *w*/w) injectable ISFI formulation, a total of ~2.2 mL would be required as a subcutaneous or intramuscular administration. Formation of PSIs by phase inversion of an ISFI formulation results in solvent-free solid implants (Fig. 5A-1); however, a large size implant (e.g. 10 mm OD/50 mm length) would be required in order to accommodate 600 mg of DTG (Supplementary Fig. 5A). Using a direct compression method combined with phase inversion (Fig. 5A), 600 mg translational dose of DTG can be formulated in a small and compact PSI implant (e.g. 10 mm OD/9 mm thickness (Supplementary Fig. 5B) or 4 mm OD/56 mm length similar to the Nexplanon® implant size for 1000 mg PSI). This dose can be further increased using larger size implants (e.g., 40 mm × 4 mm rod shaped) similar to existing marketed products (e.g., Nexplanon®) (Schlesinger et al., 2016; Barrett et al., 2018). Starting with 250 mg/g DTG in a 1:6 w/w PLGA:(NMP/DMSO) ISFI formulation, the resulting DTG concentration in the micronized DTG-PLGA powder formed by phase inversion was ~650 mg/g determined by HPLC analysis (Supplementary Fig. 5C). Using this micronized DTG-PLGA powder, the final mouse size PSI (5 mm OD/0.87 mm thickness, 20 mg) used for in vitro release studies and fabricated by direct compression contained 12.4 mg (~65 wt%) DTG. Importantly, using a direct compression process, PSIs can be produced with a wide range of drug loading (7–85 wt% DTG) by adjusting drug loading in the initial ISFI formulation (Supplementary Fig. 5D).

DSC analyses of pure DTG, placebo PSIs, and DTG PSIs (600 mg/g DTG) were carried out to determine the physical state and melting temperature of DTG in PSIs compared to its pure form. TGA analysis was conducted prior to DSC analysis to determine the decomposition temperature of DTG which was ~325 °C (Supplementary Fig. 6). As shown in Fig. 5B, pure DTG had a sharp endothermic peak at 189 °C corresponding to the melting temperature of DTG. The melting peak of DTG when formulated in the PSI was substantially smaller in intensity due to partial conversion of DTG to an amorphous state when formulated in PSI samples compared to a fully crystalline pure DTG. Moreover, the melting temperature of DTG in the PSI was similar to pure DTG (~182 °C) indicating that DTG remained stable when formulated in a PSI (Fig. 5B).

SEM imaging analyses were carried out as a corroborative method to analyze drug microstructure and physical state in the micronized powder precursor used to generate PSIs by the compression method. As shown in Fig. 5C, DTG was mostly blended with PLGA (#) in the micronized DTG-PLGA powder with presence of a small percentage of DTG in a crystalline state (*) similar to those of pure DTG (Fig. 5C).

3.2.2. PSIs mechanical properties and microstructure

Mechanical properties that allow proper handling and use of solid implants are essential to ensure good device performance. Placebo PSIs were prepared using three different compression forces (0.5, 1.0, and 1.5 US.ton, 10-mm diameter), and the Young's modulus and fracture strength of the resulting PSIs were measured. Fracture strength measures the maximum load (stress) that a solid implant can handle before it fractures. Results showed that the fracture strength of PSIs was inversely proportional to the compression force applied in the fabrication process.

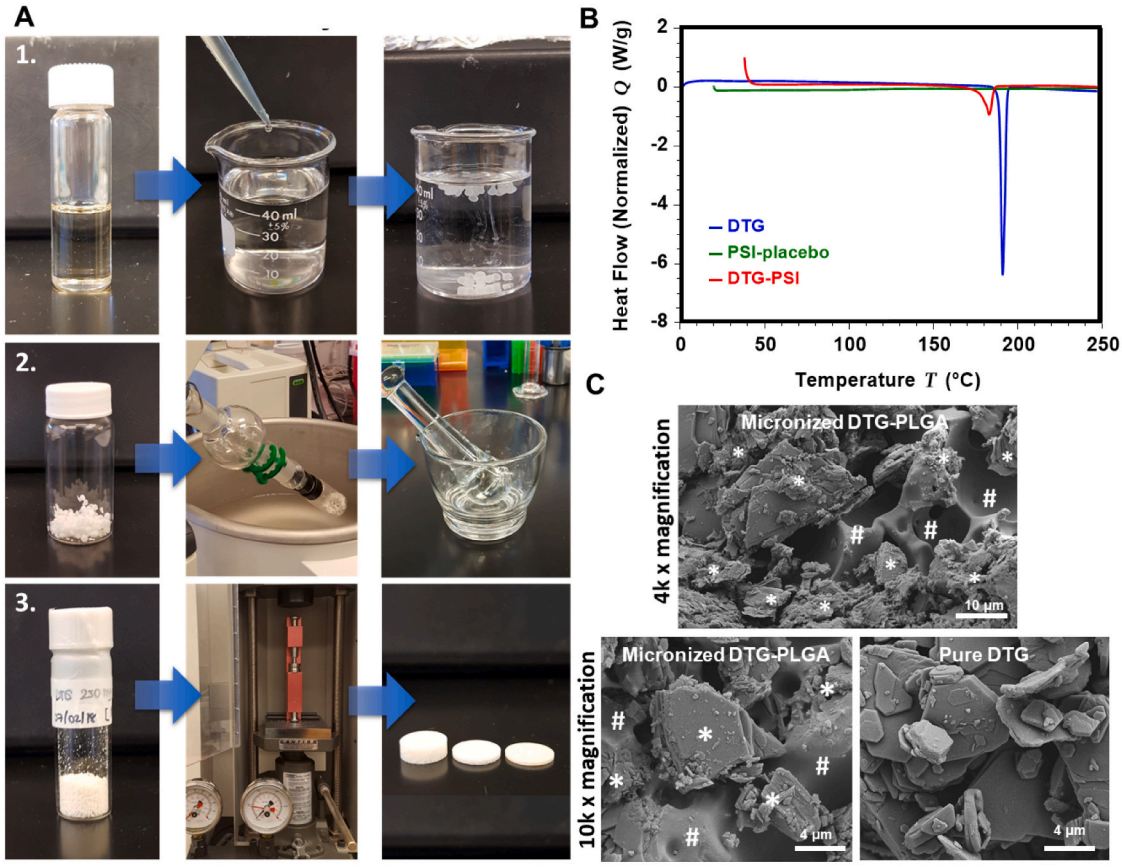

Fig. 5. Preparation and characterization of DTG PSIs. A) Fabrication process of PSIs by phase inversion and direct compression using a benchtop tablet press: (1) Preparation of ISFI formulation and solid depot by phase inversion; (2) Removal of residual solvent and micronization of dried solid depots; (3) Compression of micronized DTG-PLGA powder to form DTG PSIs. B) DSC thermograms of pure DTG, placebo PSIs, and DTG PSIs. C) SEM images of a micronized DTG-PLGA powder and pure DTG. The white * and # symbols represent DTG and PLGA respectively in the micronized DTG-PLGA powder.

The highest fracture strength (60 MN/m^2) was recorded for PSIs fabricated with the lowest compression force (0.5 US.ton), compared to 55 MN/m^2 ($p < 0.01$) and 45 MN/m^2 ($p < 0.01$) for PSIs fabricated with 1 US.ton and 1.5 US.ton respectively (Fig. 6A).

The Young's modulus measures the resistance of a solid implant to elastic deformation under a specific load and its ability to recover its original shape once the stress force is removed. Results showed that PSIs fabricated with higher compression force (1.5 US.ton) were stiffer and had a higher Young's modulus (50 MPa) compared to 42 MPa ($p < 0.01$) and 38 MPa ($p < 0.01$) for PSIs fabricated with lower compression forces (1 US.ton and 0.5 US.ton respectively) (Fig. 6B). Analyzing the microstructure of PSIs using SEM imaging demonstrated that using higher compression forces resulted in denser and more compact PSIs (Fig. 6C). This data is in agreement with the higher Young's modulus (50 MPa) obtained with the more compact, and hence, stiffer PSIs fabricated at the highest compression force (1.5 US.ton). This data also demonstrates that PSIs fabricated with different compression forces exhibit mechanical properties similar to clinically used solid implants (Kerin et al., 1998; Stewart et al., 2020).

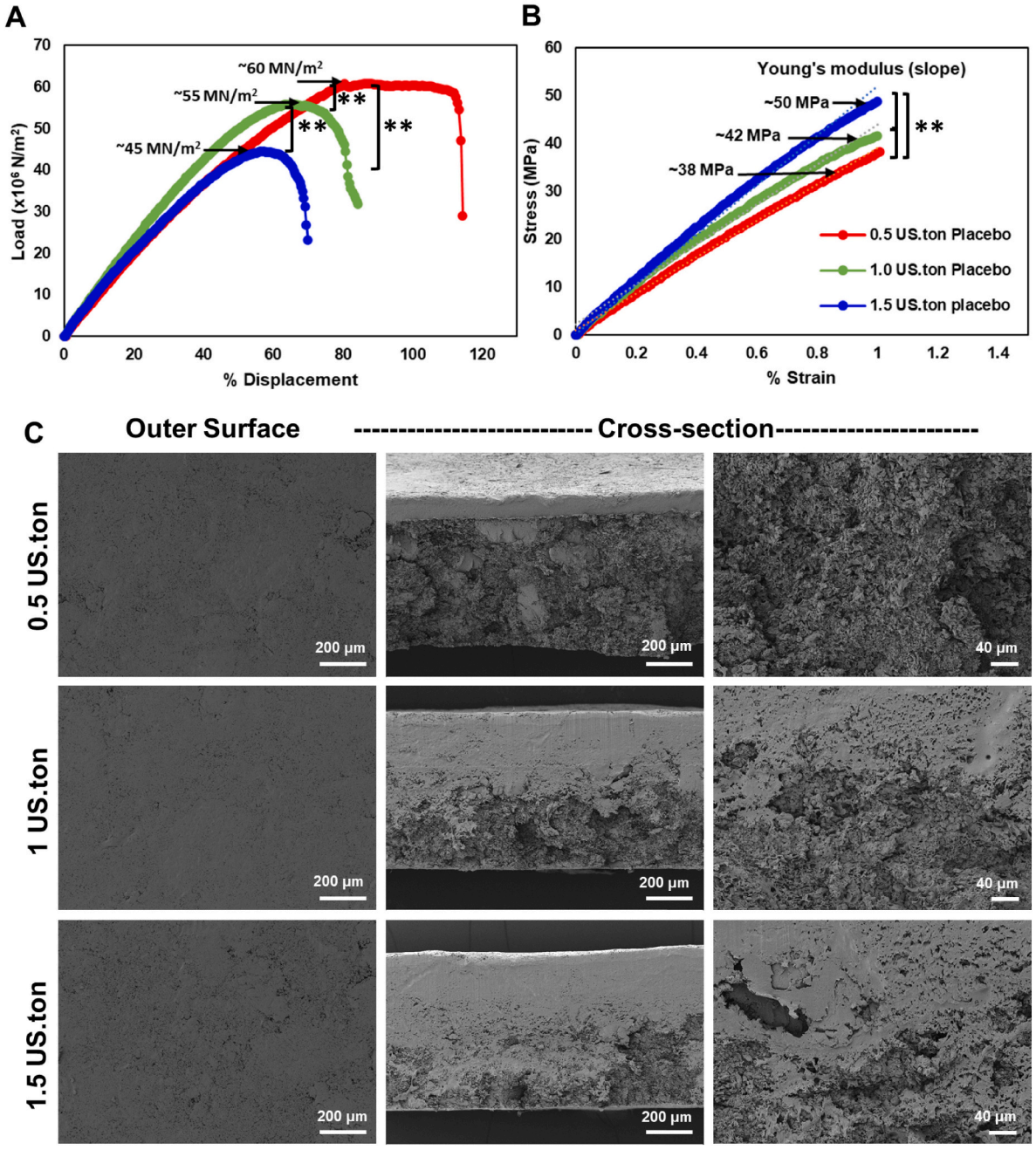

Fig. 6. PSI mechanical testing and microstructure of PSIs. The mechanical properties of placebo PSI tablets (10 mm diameter) fabricated with various compression forces (0.5, 1, and 1.5 US.ton) were evaluated. (A) Fracture strength of placebo PSIs measured using a three-point bending test with a 35 N load cell and at 0.05 mm/s displacement rate until fracture. (B) Young's modulus of PSIs calculated from the three-point bending compression test stress/strain slopes. Statistical analysis: ANOVA with Tukey's multiple comparisons tests, $^{**}p < 0.01$. C) SEM images representing cross-section images of placebo PSIs fabricated with varying compression forces.

3.3. Effects of PSI formulation parameters on in vitro release kinetics

3.3.1. Effect of PLGA molecular weight

PLGA molecular weight (MW) can be used to fine-tune drug release kinetics from PLGA-based delivery systems (Jalil and Nixon, 1990; Ogawa et al., 1988; Jain et al., 2000). In general, for PLGA-based solid implants, drug release in the initial phase, within the first 30 days, is mainly governed by a diffusion mechanism and is not influenced by the

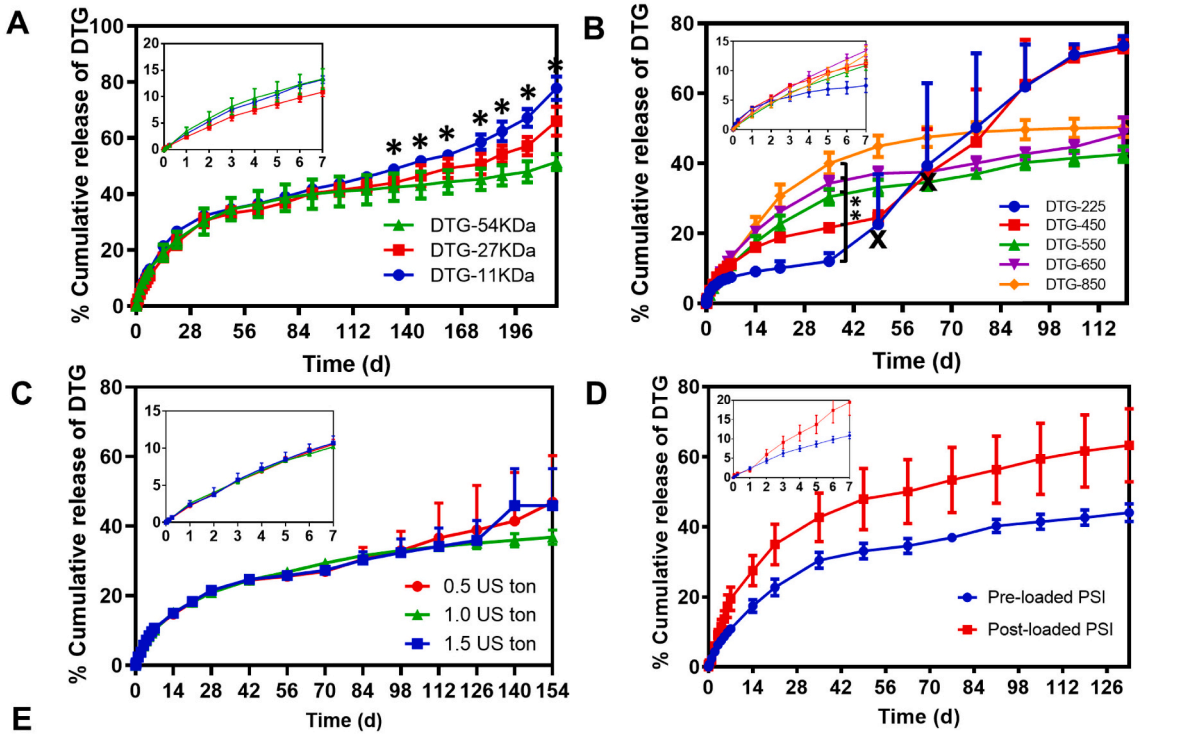

E

PSI	DTG per PSI (mg/g)	DTG per PSI (wt%)	% DTG burst at 24 h	DTG burst at 24 h (μg)	DTG release rate at zero order kinetics (μg/day)	Predicted time to 100% release (day)*
DTG-11KDa	568.21 ± 9.17	56.82 ± 0.92	3.01 ± 0.17	339.86 ± 12.30	27.53 (R^2 = 0.9554)	333
DTG-27KDa	576.60 ± 13.05	57.66 ± 1.30	2.42 ± 0.39	273.58 ± 41.94	16.09 (R^2 = 0.9805)	442
DTG-54KDa	568.78 ± 16.95	56.88 ± 1.70	3.52 ± 0.70	376.00 ± 55.28	10.36 (R^2 = 0.9687)	813
DTG-850	845.60 ± 49.91	84.56 ± 4.99	2.75 ± 0.80	429.00 ± 23.59	162.75 (R^2 = 0.9725)	1197
DTG-650	643.10 ± 28.40	64.31 ± 2.84	2.87 ± 0.37	362.28 ± 0.81	102.31 (R^2 = 0.9747)	489
DTG-550	576.60 ± 13.05	57.66 ± 1.31	2.42 ± 0.39	273.57 ± 41.94	77.72 (R^2 = 0.9836)	442
DTG-450	455.27 ± 22.59	45.53 ± 2.26	3.64 ± 0.31	316.69 ± 33.93	22.44 (R^2 = 0.9644)	149
DTG-225	218.04 ± 11.83	21.80 ± 1.18	3.56 ± 0.33	154.40 ± 13.28	6.81 (R^2 = 0.9820)	147
0.5 US ton	647.79 ± 39.15	64.78 ± 3.92	2.22 ± 0.17	432.22 ± 33.70	76.34 (R^2 = 0.9572)	530
1.0 US ton	674.86 ± 24.97	67.49 ± 2.50	2.58 ± 0.36	516.40 ± 73.00	74.40 (R^2 = 0.9690)	570
1.5 US ton	647.79 ± 39.15	64.78 ± 3.92	2.37 ± 0.53	463.94 ± 106.0	75.73 (R^2 = 0.9910)	554
Pre-loaded PSI	576.60 ± 13.05	57.66 ± 1.30	2.42 ± 0.39	273.58 ± 1.94	16.09 (R^2 = 0.9805)	442
Post-loaded PSI	551.47 ± 134.44	55.15 ± 13.44	6.00 ± 1.27	511.53 ± 8.61	18.85 (R^2 = 0.9906)	320

* The predicted time to 100% release was calculated using the extrapolated second-phase zero-order kinetics equation.

Fig. 7. Effect of PLGA MW, DTG loading and pre or post loading on the in vitro release kinetics of DTG. A) Release kinetics of DTG from PSIs fabricated with varying PLGA molecular weight (MW 11 kDa, 27 kDa, 54 kDa). DTG loading was held constant at ~570 mg/g in all PSIs. Error bars represent standard deviation of $n = 3$ samples. Statistical analysis: ANOVA with Tukey's multiple comparisons tests, $^*p < 0.05$. B) Release kinetics of DTG from PSIs fabricated with various DTG loading (225, 450, 550, 650, and 850 mg/g). Error bars represent standard deviation of n = 3 samples. The 'x' in the graph represents the timepoint at which PSIs (DTG-225 and DTG-450) significantly swelled and changed in size. Statistical analysis: ANOVA with Tukey's multiple comparisons tests, $^{**}p < 0.01$. C) Release kinetics of DTG from PSIs fabricated with varying compression forces (0.5, 1.0, 1.5 US.ton). DTG concentration was held constant at 650 mg/g. Error bars represent standard deviation of n = 3 samples. D) Release kinetics of DTG from PSIs fabricated by pre-loading method and post-loading method. DTG concentration was held constant at 650 mg/g. Error bars represent standard deviation of n = 3 samples. E) Summary of release kinetics including initial burst release and zero-order release rate for PSIs described in A-D.

molecular weight (MW) of PLGA. The effect of PLGA MW becomes more significant once the bulk degradation of PLGA by ester hydrolysis is initiated. Higher PLGA MW generally results in slower bulk degradation of the polymer backbone (Jain, 2000; Zhou et al., 1998). Our results showed no significant difference in DTG release kinetics for PSIs made with different PLGA MWs (11, 27 and 54 kDa) over 120 days (Fig. 7A, E). This result can be attributed to the densely packed PSI tablets in combination with the hydrophobic nature of DTG, which can limit water diffusion and slow the ester hydrolysis of PLGA. The effect of PLGA MW became significant ($p < 0.05$) after 133 days of incubation in PBS at 37 °C. At day 217 (last time point analyzed), DTG release reached 78% in PSIs made with the lowest PLGA MW (11 kDa) compared to 66% and 51% with 27 kDa and 54 kDa PLGA MWs respectively (Fig. 7A, E).

3.3.2. Effect of drug loading

To investigate the effect of drug loading on release kinetics, DTG PSIs were prepared with various DTG concentrations (225, 450, 550, 650, and 850 mg/g) by varying DTG concentration in the initial 1:6 *w*/w PLGA/(NMP:DMSO) ISFI formulations. Results showed that all PSIs exhibited minimum burst release of DTG in the first 24 h (~3%). The release kinetics of DTG increased with increasing drug loading in the PSIs within the first 30 days (Fig. 7B, E). PSIs containing higher DTG/PLGA weight ratios exhibited greater DTG distribution throughout the implant, which resulted in faster release kinetics. DTG PSIs with the highest DTG loading (850 mg/g, 85 wt% DTG) reached 40% release at day 35 (162.75 μg/day DTG) compared to 34% (102.31 μg/day DTG), 30% (77.72 μg/day DTG), 23% (22.44 μg/day DTG) and 6% (6.81 μg/day DTG) for 650 (65 wt% DTG), 550 (55 wt% DTG), 450 (45 wt% DTG) and 225 mg/g (22.5 wt% DTG) PSIs respectively ($p < 0.01$). The effect of drug loading on PSI swelling properties and drug release kinetics was significant after ~35 days incubation at 37 °C. This effect was observed with PSIs that had the two lowest DTG content (22.5 wt% and 45 wt% DTG), which resulted in a significant increase in DTG release rate on day 49 (6.81 μg/day to 39.47 μg/day, $p < 0.01$) for the 225 mg/g (22.5 wt%) DTG PSI and on day 63 (22.44 μg/day to 72.79 μg/day, $p < 0.01$) for the 450 mg/g (45 wt%) DTG PSI (Fig. 7B). Interestingly, PSIs that contained higher DTG concentrations (>50 wt%) did not exhibit this same effect and maintained sustained release kinetics over 120 days (Fig. 7B, E). These results demonstrate that drug release kinetics and release duration can be fine-tuned and controlled by varying drug loading within the PSIs (Fig. 7E). These results also demonstrate that for release durations beyond 30 days, drug loading in PSIs had a significant effect on the release kinetics.

3.3.3. Effect of compression force

The effect of compression force in the PSI fabrication process on DTG release kinetics was investigated. DTG PSIs prepared by different compression forces (0.5, 1.0 and 1.5 US.ton, 10-mm diameter) were prepared with a constant DTG concentration (650 mg/g). Results showed no significant effect of compression force used in the fabrication process on DTG release from the various PSIs (Fig. 7C, E). All PSIs reached ~35% release at day 112 and had similar DTG release rate (~75 μg/day DTG) within zero-order release kinetics. These results demonstrate that the mechanical properties of drug loaded PSIs can be optimized by the applied compression force independently of drug release kinetics.

3.3.4. Effect of drug incorporation process

Fabrication of drug-loaded PSIs can be done by either incorporating drug(s) in the initial ISFI formulation (termed pre-loading) or by adding drug(s) to a micronized polymer powder (termed post-loading). We sought out to investigate the effect of drug incorporation step on in vitro release kinetics from PSIs. Results demonstrated that in PSIs where DTG was added using the pre-loading method, DTG exhibited slower and more sustained release kinetics over 130 days (16.09 μg/day DTG from d30-d130) (Fig. 7D, E). In PSIs where DTG was added using the post-loading method, the release kinetics were faster (18.85 μg/day DTG from d30-d130, $p < 0.05$ (Cohen et al., 2013)) and had greater variability, which could be attributed to lower homogeneity in drug distribution within the PSIs using the post-loading method.

3.4. Accelerated stability studies

The stability of DTG in the DTG PSIs was determined under accelerated stability storage conditions (40 °C and 75% RH) for 6 months. DTG remained chemically stable in the PSIs for 6 months with no change in loading concentration and no presence of degradation peaks as determined by HPLC analysis (Fig. 8A, C). DTG PSIs were also monitored for changes in appearance, color, or size. No change in physical appearance or size was observed after 0, 14, 30, 90 or 180 days of storage at 40 °C/75% RH storage conditions (Fig. 8B).

3.5. DTG activity in PSIs

Effect of PSI fabrication on activity of DTG was evaluated in DTG-PSI stored for 6 months at 40 °C/75%RH. DTG was eluted from PSI in PBS. The HIV inhibitory activity of DTG was determined as the half maximal inhibitory concentration (IC50) using TZM-bl indicator cells. The IC50 of DTG eluted from the implant (0.6 ng/ml) was not significantly different from the activity of DTG in freshly prepared solution (Fig. 9) and consistent with DTG IC50 reported in TZM-bl cells (Anstett et al., 2015; Liang et al., 2015).

4. Discussion

Developing biodegradable polymer-based implants that can provide sustained drug delivery over several months after a single administration is an area of high demand and importance in a number of medical applications. PLGA is one of the most widely used polymers in formulation development and drug delivery systems, including solid implants (Jain, 2000; Widmer et al., 1998a; Makadia and Siegel, 2011; Lee and Pokorski, 2018). Up until now, PLGA solid implants have been manufactured by hot-melt extrusion, (Widmer et al., 1998b; Wang et al., 2010) solvent-casting (Siegel et al., 2002) or compression molding (Rabin et al., 2008; Siegel et al., 2006). These methods have several limitations, including required high heat, high pressure or use of large volumes of organic solvents, which limit the type of drugs that can be formulated or the scalability of the process. Herein, we report for the first time a manufacturing process of PLGA solid implants that does not require high heat, high pressure or large volumes of organic solvents. This process combines a phase inversion and micronization process to form a solvent-free drug loaded powder, which is then used to form a solid implant using tablet compression. The final implant can be engineered with different shapes or sizes to accommodate required drug release kinetics and improve patient compliance. In this process, drug loading can be accomplished in two ways either by incorporating a drug in the initial ISFI formulation prior to the phase inversion step or by incorporating a drug in a preformed micronized PLGA powder after the phase inversion step. Our results showed that loading DTG in the initial ISFI formulation prior to phase inversion resulted in PSIs that exhibited more controlled and sustained DTG release. This drug loading process also afforded high drug loading capacity up to 85 wt% DTG in PSIs. Direct compression allows the fabrication of highly compact solid implants with high percent drug loading (up to 85 wt% DTG) in the final PSI (Supplementary Fig. 5D). As a result, DTG PSIs can be fabricated to accommodate a translational dose of ≥600 mg (Murray et al., 2018; Clement et al., 2020) in a single rod-shaped implant with a dimension of 4 mm OD/56 mm length similar to existing marketed products (e.g., Nexplanon®), which can accommodate a DTG dose of 1000 mg/implant (Schlesinger et al., 2016; Barrett et al., 2018).

The physical state of DTG assessed by DSC and SEM showed that DTG was semi-crystalline and stable when formulated in PSIs and distributed

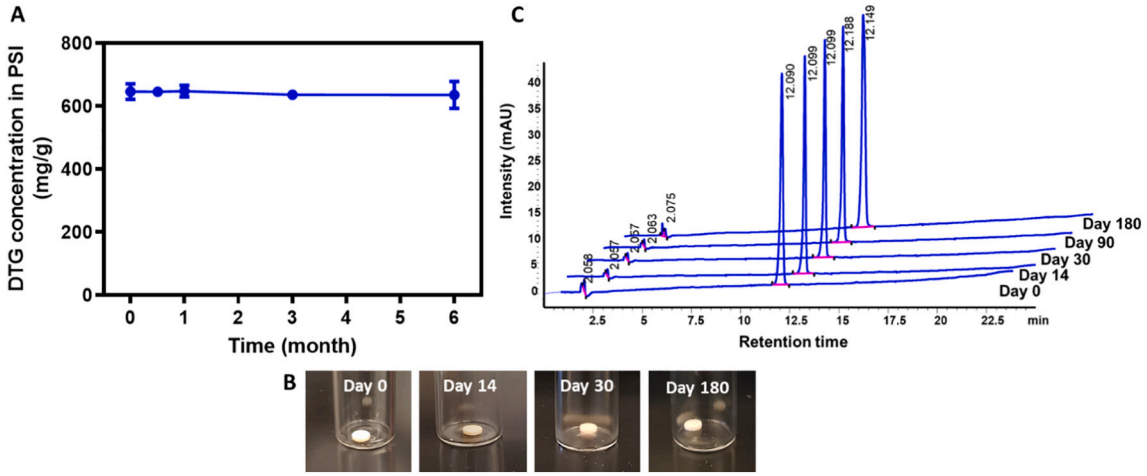

Fig. 8. Accelerated stability studies of DTG PSIs. A) DTG concentration in PSIs before (day 0) and after storage at 40 °C and 75% RH for 14, 30, 90, and 180 days. B) Physical appearance of the DTG PSIs before (day 0) and after storage at 40 °C and 75% RH for 14, 30, 90, and 180 days. C) HPLC chromatograms of DTG extracted from PSIs before (day 0) and after storage at 40 °C and 75% RH for 14, 30, 90, and 180 days.

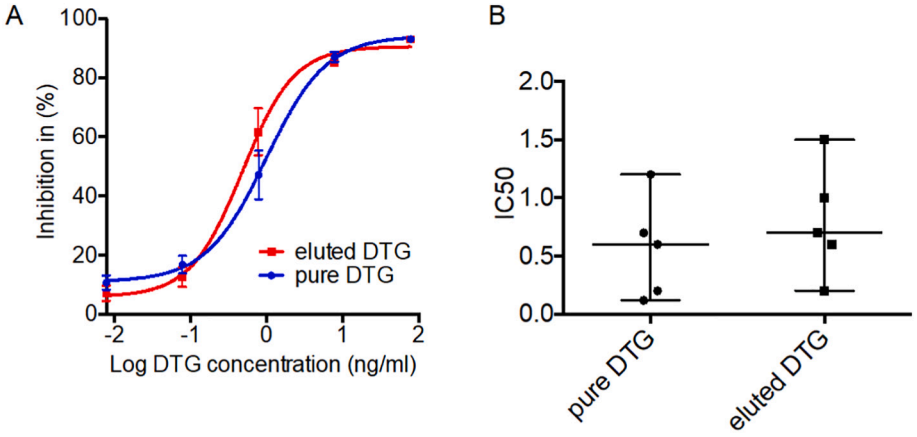

Fig. 9. DTG activity in PSI. DTG ability to inhibit HIV was determined in TZM-bl indicator cells with a luciferase reporter gene. Results were normalized to the luciferase activity of cells infected with HIV in the absence of DTG. Inhibitory activity of DTG was expressed as a percentage of decrease in luciferase activity. (A) inhibitory activity of eluted (red) and pure (blue) DTG, data was fitted to a sigmoid dose-response curve, each dilution measured in quadruplicates. Mean ± S.E.M. shown. (B) IC50, mean ± standard error of the mean (S.E.M) are shown.

homogenously within the solid implant prepared by phase inversion, micronization and compression (Fig. 5). However, the distribution of DTG in PSIs prepared by phase inversion of ISFI formulation was variable and controlled solely by the rate of phase inversion (Fig. 3). Specifically, with higher content of NMP solvent (lower PLGA:NMP), the rate of phase inversion was faster and left behind the majority of drugs in the core of the solid implant (Fig. 3C). Accelerated stability studies showed that DTG retained its physical and chemical properties in the PSI for 6 months when stored at 40 °C/75%RH, with no change in drug concentration or degradation over time. Moreover, DTG activity based on its ability to inhibit HIV infection of TZM-bl cells was maintained post storage of DTG PSIs at 40 °C/75%RH for 6 months, demonstrating the long-term stability of DTG in the PSIs.

In vitro release studies of DTG from PSIs demonstrated the ability to fine-tune the release kinetics of DTG by varying shape of PSI, initial ratio of PLGA:NMP in ISFI formulation, PLGA molecular weight (MW) or by changing drug loading in the PSI (Schliecker et al., 2003; Frank et al., 2005; Grizzi et al., 1995; Lu et al., 2000). The surface area of a PSI is depended on the shape of the PSI. PSI with higher surface area resulted in faster release kinetics because it allows the faster drug diffusion and higher water penetration (Fig. 2). Additionally, the release kinetics of drugs from a PSI can be tuned based on the initial ratio of PLGA:NMP in the precursor ISFI formulation. Higher ratio of PLGA:NMP resulted in higher percentage of PLGA in the PSI matrix leading to slower release kinetics (Fig. 3). In other words, higher ratio of PLGA:NMP resulted in lower percentage of DTG in the final PSI leading to slower release kinetics. Although the use of co-solvent in the initial ISFI formulation can enhance drug loading (3 wt% in PSI), this 3% increase of DTG loading was not sufficient to alter the release kinetics of DTG. Furthermore, higher MW PLGA resulted in slower DTG release kinetics beyond day ~130, and higher drug loading resulted in faster release kinetics of DTG within the first phase (d1-35) of release (Fig. 7). Moreover, all PSIs resulted in sustained release of DTG for 6 months or longer and minimum burst in the first 24 h (<6%). DTG concentrations released in vitro from various PSIs were above the 4×PAIC90 of DTG (4×64 ng/mL), which is a known benchmark concentration for antiretroviral drugs to achieve efficacy in HIV prevention (Fig. 7) (Adams et al., 2013; Radzio et al., 2015; Andrews et al., 2014). In general, DTG release from PSIs followed a biphasic release profile with an initial faster zero-order release within the first 30–35 days mainly driven by a drug diffusion mechanism. In the second phase, where drug release is mainly a result of PLGA bulk degradation initiated via ester hydrolysis after ~30–35 days of incubation at 37 °C, DTG exhibited a slower release rate (Fig. 7). PSIs with DTG loading <50 wt% had a third phase with significantly higher release rates due to swelling of PSIs after extended incubation times (>45 days) in PBS at 37 °C (Fig. 7B). PSI swelling facilitates diffusion of water into the implant and results in PLGA bulk degradation via ester hydrolysis leading to faster DTG release kinetics. The inability to provide an absolute zero-order in vitro release kinetics could present a limitation for this technology, should a similar trend be observed in vivo,

compared to other LA solid implant technologies currently in development such as non-biodegradable EVA implants (Barrett et al., 2018), and nanofluidic devices for HIV prevention (Chua et al., 2018; Pons-Faudoa et al., 2020). However, it should be noted that the swelling behavior observed when evaluating these PSIs in vitro and which mainly contributed to the bi-phasic nature of the release profiles, is likely an artifact of incubating the PSIs in a large volume (200 mL) of release medium in order to maintain sink conditions during the in vitro release studies. This swelling behavior will likely be significantly reduced in vivo due to much smaller volumes of fluids in a subcutaneous space compared to the large volume used in the in vitro release studies.

Modifying the mechanical properties of the PSIs did not influence the release kinetics of DTG. PSIs fabricated with varying compression forces (0.5, 1.0 or 1.5 US.ton) and loaded with a constant DTG concentration (650 mg/g) all showed similar release kinetics (Fig. 7C). All PSIs exhibited high fracture strength in the range of 45–60 MN/m^2, which is comparable to the fracture strength of cartilage (Kerin et al., 1998), indicating that the PSIs have the right properties to maintain their structural integrity in vivo. Collectively, these data demonstrate the flexibility of the PSIs to achieve sustained target release kinetics and drug concentrations that can be translated to humans.

5. Conclusions

PSIs were successfully fabricated using a novel process that combines polymer phase inversion and compression. This process generated PSIs with high drug loading (up to 85 wt%) and provided ultra-long-acting drug release for 6 months or longer in vitro. Drug release kinetics can be fine-tuned by various methods, including device surface area (i.e. shape/size), formulation compositions (polymer MW or type), and drug loading concentration. Optimization of PSI mechanical properties can be done independently of drug release kinetics. Drug loaded PSIs were stable under accelerated stability storage conditions over six months, and dolutegravir (DTG) retained its physical and chemical properties as well as its potency (IC50) to inhibit HIV infection. To our knowledge, this is the first report on a PLGA-based solid implant that can be fabricated by a phase inversion and compression process. This process does not require high heat, high pressure or use of high volumes of organic solvents and can be easily scalable to produce solid implants with high drug loading and various shapes or sizes. This technology can also be used with other polymers (e.g. poly(lactic acid), PLA) and a wide range of drugs including drugs that are sensitive to high heat or pressure and cannot be formulated by extrusion or compression molding to expand its application for a wide range of indications. Ongoing studies are investigating formulations of multiple drugs in a single PSI and in vivo safety and pharmacokinetic studies.

Author contributions

The manuscript was written through contributions of all authors. All authors have given approval to the final version of the manuscript.

Authors statement

Conceived and designed the experiments: SRB, PM, MK, and JVG.

Performed the experiments: PM, GP, and MK. Analyzed the data: SRB, PM, GP, MK and JVG.

Contributed reagents/materials/analysis tools: SRB, MK, and JVG.

Wrote the paper: SRB, PM, MK, and JVG.

Declaration of Competing Interest

SRB, PM, MK and JVG are inventors on a patent application related to this work filed by the University of North Carolina, Office of Technology Commercialization (UNC OTC) (PCT International Application PCT/US20/16061, filed on January 31, 2020 and U.S. Provisional Patent Application No. 62/800087 filed on February 6, 2019). The authors declare no competing financial interest.

The authors declare that they have no known competing financial interests or personal relationships that could have appeared to influence the work reported in this paper

Acknowledgements

This work was supported by National Institute of Allergy and Infectious Diseases (grant numbers R01AI131430 to MK and RB, R01AI073146 and R01AI096138 to JVG). This work was also supported by the UNC CFAR (P30 AI050410). The content is solely the responsibility of the authors and does not necessarily represent the official views of the National Institute of Allergy and Infectious Diseases.

Appendix A. Supplementary data

Supplementary data to this article can be found online at https://doi.org/10.1016/j.ijpx.2020.100068.

References

Adams, J.L., Patterson, K.B., Prince, H.M.A., Sykes, C., Greener, B.N., Dumond, J.B., Kashuba, A.D.M., 2013. Single and multiple dose pharmacokinetics of dolutegravir in the genital tract of HIV-negative women. Antivir. Ther. 18 (8), 1005–1013.

Affandi, B., Santoso, S., Hadisaputra, W., Moeloek, F., Prihartono, J., Lubis, F., Samil, R., 1987. Five-year experience with Norplant®. Contraception 36 (4), 417–428.

Alderks, C.E., 2013. Trends in the Use of Methadone, Buprenorphine, and Extended-Release Naltrexone at Substance Abuse Treatment Facilities: 2003–2015 (Update), the CBHSQ Report, Substance Abuse and Mental Health Services Administration (US), Rockville (MD), pp. 1–8.

Andrews, C.D., Spreen, W.R., Mohri, H., Moss, L., Ford, S., Gettie, A., Russell-Lodrigue, K., Bohm, R.P., Cheng-Mayer, C., Hong, Z., Markowitz, M., Ho, D.D., 2014. Long-acting integrase inhibitor protects macaques from intrarectal simian/human immunodeficiency virus. Science 343 (6175), 1151–1154.

Anstett, K., Mesplede, T., Oliveira, M., Cutillas, V., Wainberg, M.A., 2015. Dolutegravir resistance mutation R263K cannot coexist in combination with many classical integrase inhibitor resistance substitutions. J. Virol. 89 (8), 4681–4684.

Baert, L., van t Klooster, G., Dries, W., François, M., Wouters, A., Basstanie, E., Iterbeke, K., Stappers, F., Stevens, P., Schueller, L., Van Remoortere, P., Kraus, G., Wigerinck, P., Rosier, J., 2009. Development of a long-acting injectable formulation with nanoparticles of rilpivirine (TMC278) for HIV treatment. Eur. J. Pharm. Biopharm. 72 (3), 502–508.

Barnwal, P., Das, S., Mondal, S., Ramasamy, A., Maiti, T., Saha, A., 2017. Probuphine® (buprenorphine implant): a promising candidate in opioid dependence. Therap. Adv. Psychopharmacol. 7 (3), 119–134.

Barrett, S.E., Teller, R.S., Forster, S.P., Li, L., Mackey, M.A., Skomski, D., Yang, Z., Fillgrove, K.L., Doto, G.J., Wood, S.L., Lebron, J., Grobler, J.A., Sanchez, R.I., Liu, Z., Lu, B., Niu, T., Sun, L., Gindy, M.E., 2018. Extended-Duration MK-8591-Eluting implant as a candidate for HIV treatment and prevention. Antimicrob. Agents Chemother. 62 (10) e01058-18.

Benhabbour, S.R., Kovarova, M., Jones, C., Copeland, D.J., Shrivastava, R., Swanson, M. D., Sykes, C., Ho, P.T., Cottrell, M.L., Sridharan, A., Fix, S.M., Thayer, O., Long, J.M., Hazuda, D.J., Dayton, P.A., Mumper, R.J., Kashuba, A.D.M., Victor Garcia, J., 2019. Ultra-long-acting tunable biodegradable and removable controlled release implants for drug delivery. Nat. Commun. 10 (1), 4324.

Branum, A.M., Jones, J., 2015. Trends in long-acting reversible contraception use among U.S. women aged 15-44. NCHS Data Brief 188, 1–8.

Bunge, K.E., Dezzutti, C.S., Rohan, L.C., Hendrix, C.W., Marzinke, M.A., Richardson-Harman, N., Moncla, B.J., Devlin, B., Meyn, L.A., Spiegel, H.M.L., Hillier, S.L., 2016. A phase 1 Trial to Assess the Safety, Acceptability, Pharmacokinetics, and Pharmacodynamics of a Novel Dapivirine Vaginal Film. J. Acquired Immune Deficien. Syndrom. (1999) 71 (5), 498–505.

Chua, C.Y.X., Jain, P., Ballerini, A., Bruno, G., Hood, R.L., Gupte, M., Gao, S., Di Trani, N., Susnjar, A., Shelton, K., Bushman, L.R., Folci, M., Filgueira, C.S., Marzinke, M.A., Anderson, P.L., Hu, M., Nehete, P., Arduino, R.C., Sastry, J.K., Grattoni, A., 2018. Transcutaneously refillable nanofluidic implant achieves sustained level of tenofovir diphosphate for HIV pre-exposure prophylaxis. J. Control. Release 286, 315–325.

Clement, M.E., Kofron, R., Landovitz, R.J., 2020. Long-acting injectable cabotegravir for the prevention of HIV infection. Curr. Opin. HIV AIDS 15 (1).

Cohen, J., Cohen, P., West, S.G., Aiken, L.S., 2013. Applied Multiple Regression/Correlation Analysis for the Behavioral Sciences. Routledge.

Dammerman, R., Kim, S., Adera, M., Schwarz, A., 2018. Pharmacokinetics and safety of risperidone subcutaneous implants in stable patients with schizophrenia. Clin. Pharmacol. Drug development 7 (3), 298–310.

Dash, A., Cudworth II, G., 1998. Therapeutic applications of implantable drug delivery systems. J. Pharmacol. Toxicol. Methods 40 (1), 1–12.

Date, A.A., Shibata, A., Goede, M., Sanford, B., La Bruzzo, K., Belshan, M., Destache, C.J., 2012. Development and evaluation of a thermosensitive vaginal gel containing raltegravir+ efavirenz loaded nanoparticles for HIV prophylaxis. Antivir. Res. 96 (3), 430–436.

Devlin, B., Nuttall, J., Wilder, S., Woodsong, C., Rosenberg, Z., 2013. Development of dapivirine vaginal ring for HIV prevention. Antivir. Res. 100, S3–S8.
Dinunzio, J.C., Brough, C., Hughey, J.R., Miller, D.A., Williams 3rd, R.O., McGinity, J.W., 2010. Fusion production of solid dispersions containing a heat-sensitive active ingredient by hot melt extrusion and Kinetisol dispersing. Eur. J. Pharm. Biopharm. 74 (2), 340–351.
Elstad, N.L., Fowers, K.D., 2009. OncoGel (ReGel/paclitaxel)—Clinical applications for a novel paclitaxel delivery system. Adv. Drug Deliv. Rev. 61 (10), 785–794.
Fetherston, S.M., Boyd, P., McCoy, C.F., McBride, M.C., Edwards, K.-L., Ampofo, S., Malcolm, R.K., 2013. A silicone elastomer vaginal ring for HIV prevention containing two microbicides with different mechanisms of action. Eur. J. Pharm. Sci. 48 (3), 406–415.
Frank, A., Rath, S.K., Venkatraman, S.S., 2005. Controlled release from bioerodible polymers: effect of drug type and polymer composition. J. Control. Release 102 (2), 333–344.
Fu, Y., Kao, W.J., 2010. Drug release kinetics and transport mechanisms of non-degradable and degradable polymeric delivery systems. Expert Opin. Drug Deliv. 7 (4), 429–444.
García-Lerma, J.G., Heneine, W., 2012. Animal models of antiretroviral prophylaxis for HIV prevention. Curr. Opin. HIV AIDS 7 (6), 505–513.
Glaubius, R., Ding, Y., Penrose, K.J., Hood, G., Engquist, E., Mellors, J.W., Parikh, U.M., Abbas, U.L., 2019. Dapivirine vaginal ring for HIV prevention: modelling health outcomes, drug resistance and cost-effectiveness. J. Int. AIDS Soc. 22 (5), e25282.
Goldspiel, B.R., Kohler, D.R., 1991. Goserelin acetate implant: a depot luteinizing hormone-releasing hormone analog for advanced prostate cancer. DICP 25 (7–8), 796–804.
Goyanes, A., Robles Martinez, P., Buanz, A., Basit, A.W., Gaisford, S., 2015. Effect of geometry on drug release from 3D printed tablets. Int. J. Pharm. 494 (2), 657–663.
Grammen, C., Ariën, K.K., Venkatraj, M., Joossens, J., Van der Veken, P., Heeres, J., Lewi, P.J., Haenen, S., Augustyns, K., Vanham, G., 2014. Development and in vitro evaluation of a vaginal microbicide gel formulation for UAMC01398, a novel diaryltriazine NNRTI against HIV-1. Antivir. Res. 101, 113–121.
Grizzi, I., Garreau, H., Li, S., Vert, M., 1995. Hydrolytic degradation of devices based on poly(dl-lactic acid) size-dependence. Biomaterials 16 (4), 305–311.
Guthrie, K.M., Rohan, L., Rosen, R.K., Vargas, S.E., Shaw, J.G., Katz, D., Kojic, E.M., Ham, A.S., Friend, D., Buckheit, K.W., Buckheit Jr., R.W., 2018. Vaginal film for prevention of HIV: using visual and tactile evaluations among potential users to inform product design. Pharm. Dev. Technol. 23 (3), 311–314.
Haghjou, N., Soheilian, M., Abdekhodaie, M.J., 2011. Sustained release intraocular drug delivery devices for treatment of uveitis. J. Ophtha. Vision Res. 6 (4), 317.
Haller, J.A., Dugel, P., Weinberg, D.V., Chou, C., Whitcup, S.M., 2009. Evaluation of the safety and performance of an applicator for a novel intravitreal dexamethasone drug delivery system for the treatment of macular edema. Retina 29 (1), 46–51.
Iyer, S., Radwan, A.E., Hafezi-Moghadam, A., Malyala, P., Amiji, M., 2019. Long-acting intraocular delivery strategies for biological therapy of age-related macular degeneration. J. Control. Release 296, 140–149.
Jain, R.A., 2000. The manufacturing techniques of various drug loaded biodegradable poly (lactide-co-glycolide)(PLGA) devices. Biomaterials 21 (23), 2475–2490.
Jain, R.A., Rhodes, C.T., Railkar, A.M., Malick, A.W., Shah, N.H., 2000. Controlled release of drugs from injectable in situ formed biodegradable PLGA microspheres: effect of various formulation variables. Eur. J. Pharm. Biopharm. 50 (2), 257–262.
Jalil, R., Nixon, J., 1990. Biodegradable poly (lactic acid) and poly (lactide-co-glycolide) microcapsules: problems associated with preparative techniques and release properties. J. Microencapsul. 7 (3), 297–325.
Kaplan, G., Casoy, J., Zummo, J., 2013. Impact of long-acting injectable antipsychotics on medication adherence and clinical, functional, and economic outcomes of schizophrenia. Patient Prefere. Adhere. 7, 1171–1180.
Keele, B.F., Giorgi, E.E., Salazar-Gonzalez, J.F., Decker, J.M., Pham, K.T., Salazar, M.G., Sun, C., Grayson, T., Wang, S., Li, H., Wei, X., Jiang, C., Kirchherr, J.L., Gao, F., Anderson, J.A., Ping, L.H., Swanstrom, R., Tomaras, G.D., Blattner, W.A., Goepfert, P.A., Kilby, J.M., Saag, M.S., Delwart, E.L., Busch, M.P., Cohen, M.S., Montefiori, D.C., Haynes, B.F., Gaschen, B., Athreya, G.S., Lee, H.Y., Wood, N., Seoighe, C., Perelson, A.S., Bhattacharya, T., Korber, B.T., Hahn, B.H., Shaw, G.M., 2008. Identification and characterization of transmitted and early founder virus envelopes in primary HIV-1 infection. Proc. Natl. Acad. Sci. U. S. A. 105 (21), 7552–7557.
Kerin, A.J., Wisnom, M.R., Adams, M.A., 1998. The compressive strength of articular cartilage. Proc. Inst. Mech. Eng. H J. Eng. Med. 212 (4), 273–280.
Kjome, K.L., Moeller, F.G., 2011. Long-acting injectable naltrexone for the management of patients with opioid dependence. Subst. Abus. 5, 1–9.
Kovarova, M., Council, O.D., Date, A.A., Long, J.M., Nochi, T., Belshan, M., Shibata, A., Vincent, H., Baker, C.E., Thayer, W.O., Kraus, G., Lachaud-Durand, S., Williams, P., Destache, C.J., Garcia, J.V., 2015. Nanoformulations of rilpivirine for topical pericoital and systemic coitus-independent administration efficiently prevent HIV transmission. PLoS Pathog. 11 (8), e1005075.
Kovarova, M., Benhabbour, S.R., Massud, I., Spagnuolo, R.A., Skinner, B., Baker, C.E., Sykes, C., Mollan, K.R., Kashuba, A.D.M., García-Lerma, J.G., Mumper, R.J., Garcia, J.V., 2018. Ultra-long-acting removable drug delivery system for HIV treatment and prevention. Nat. Commun. 9 (1), 4156.
Koyanagi, Y., Miles, S., Mitsuyasu, R.T., Merrill, J.E., Vinters, H.V., Chen, I.S., 1987. Dual infection of the central nervous system by AIDS viruses with distinct cellular tropisms. Science 236 (4803), 819–822.
Landovitz, R.J., Kofron, R., McCauley, M., 2016. The promise and pitfalls of long acting injectable agents for HIV prevention. Curr. Opin. HIV AIDS 11 (1), 122–128.
Lee, P.W., Pokorski, J.K., 2018. Poly(lactic-co-glycolic acid) devices: production and applications for sustained protein delivery. Wiley Interdiscip. Rev. Nanomed. Nanobiotechnol. https://doi.org/10.1002/wnan.1516.
Lee, S.-Y., Chee, S.-P., 2005. Surodex after phacoemulsification. J Cataract Refract Surg 31 (8), 1479–1480.
Liang, J., Mesplede, T., Oliveira, M., Anstett, K., Wainberg, M.A., 2015. The combination of the R263K and T66I resistance substitutions in HIV-1 integrase is incompatible with high-level viral replication and the development of high-level drug resistance. J. Virol. 89 (22), 11269–11274.
Lu, L., Peter, S.J., Lyman, M.D., Lai, H.-L., Leite, S.M., Tamada, J.A., Uyama, S., Vacanti, J.P., Robert, L., Mikos, A.G., 2000. In vitro and in vivo degradation of porous poly(dl-lactic-co-glycolic acid) foams. Biomaterials 21 (18), 1837–1845.
Macoul, K.L., Pavan-Langston, D., 1975. Pilocarpine ocusert system for sustained control of ocular hypertension. Arch. Ophthalmol. 93 (8), 587–590.
Makadia, H.K., Siegel, S.J., 2011. Poly lactic-co-glycolic acid (PLGA) as biodegradable controlled drug delivery carrier. Polymers (Basel) 3 (3), 1377–1397.
Mansour, D., 2010. Nexplanon®: what Implanon® did next. BMJ Sex. Reprod. Health 36 (4), 187.
Murray, M.I., Markowitz, M., Frank, I., Grant, R.M., Mayer, K.H., Hudson, K.J., Stancil, B. S., Ford, S.L., Patel, P., Rinehart, A.R., 2018. Satisfaction and acceptability of cabotegravir long-acting injectable suspension for prevention of HIV: patient perspectives from the ECLAIR trial. HIV Clinic. Trials 19 (4), 129–138.
Nickel, J.C., Jain, P., Shore, N., Anderson, J., Giesing, D., Lee, H., Kim, G., Daniel, K., White, S., Larrivee-Elkins, C., Lekstrom-Himes, J., Cima, M., 2012. Continuous intravesical lidocaine treatment for interstitial cystitis/bladder pain syndrome: safety and efficacy of a new drug delivery device. Sci. Transl. Med. 4 (143), 143ra100.
Ochsenbauer, C., Edmonds, T.G., Ding, H., Keele, B.F., Decker, J., Salazar, M.G., Salazar-Gonzalez, J.F., Shattock, R., Haynes, B.F., Shaw, G.M., Hahn, B.H., Kappes, J.C., 2012. Generation of transmitted/founder HIV-1 infectious molecular clones and characterization of their replication capacity in CD4 T lymphocytes and monocyte-derived macrophages. J. Virol. 86 (5), 2715–2728.
Ogawa, Y., YAMAMOTO, M., TAKADA, S., OKADA, H., SHIMAMOTO, T., 1988. Controlled-release of leuprolide acetate from polylactic acid or copoly (lactic/glycolic) acid microcapsules: influence of molecular weight and copolymer ratio of polymer. Chem. Pharm. Bull. 36 (4), 1502–1507.
Permar, S.R., Salazar, M.G., Gao, F., Cai, F., Learn, G.H., Kalilani, L., Hahn, B.H., Shaw, G.M., Salazar-Gonzalez, J.F., 2013. Clonal amplification and maternal-infant transmission of nevirapine-resistant HIV-1 variants in breast milk following single-dose nevirapine prophylaxis. Retrovirology 10, 88.
Pons-Faudoa, F.P., Ballerini, A., Sakamoto, J., Grattoni, A., 2019. Advanced implantable drug delivery technologies: transforming the clinical landscape of therapeutics for chronic diseases. Biomed. Microdevices 21 (2), 47.
Pons-Faudoa, F.P., Sizovs, A., Shelton, K.A., Momin, Z., Bushman, L.R., Xu, J., Chua, C.Y. X., Nichols, J.E., Hawkins, T., Rooney, J.F., Marzinke, M.A., Kimata, J.T., Anderson, P.L., Nehete, P.N., Arduino, R.C., Ferrari, M., Sastry, K.J., Grattoni, A., 2020. Preventive efficacy of a tenofovir alafenamide fumarate nanofluidic implant in SHIV-challenged nonhuman primates. bioRxiv 21 (47), 1–22, 2020.05.13.091694.
Rabin, C., Liang, Y., Ehrlichman, R.S., Budhian, A., Metzger, K.L., Majewski-Tiedeken, C., Winey, K.I., Siegel, S.J., 2008. In vitro and in vivo demonstration of risperidone implants in mice. Schizophr. Res. 98 (1), 66–78.
Radzio, J., Spreen, W., Yueh, Y.L., Mitchell, J., Jenkins, L., García-Lerma, J.G., Heneine, W., 2015. The long-acting integrase inhibitor GSK744 protects macaques from repeated intravaginal SHIV challenge. Sci. Transl. Med. 7 (270), 270ra5.
Rajgor, N., Patel, M., Bhaskar, V., 2011. Implantable drug delivery systems: an overview. Surg. Neurol. Int. 2 (2).
Salazar-Gonzalez, J.F., Salazar, M.G., Keele, B.F., Learn, G.H., Giorgi, E.E., Li, H., Decker, J.M., Wang, S., Baalwa, J., Kraus, M.H., Parrish, N.F., Shaw, K.S., Guffey, M. B., Bar, K.J., Davis, K.L., Ochsenbauer-Jambor, C., Kappes, J.C., Saag, M.S., Cohen, M.S., Mulenga, J., Derdeyn, C.A., Allen, S., Hunter, E., Markowitz, M., Hraber, P., Perelson, A.S., Bhattacharya, T., Haynes, B.F., Korber, B.T., Hahn, B.H., Shaw, G.M., 2009. Genetic identity, biological phenotype, and evolutionary pathways of transmitted/founder viruses in acute and early HIV-1 infection. J. Exp. Med. 206 (6), 1273–1289.
Schlesinger, E., Johengen, D., Luecke, E., Rothrock, G., McGowan, I., van der Straten, A., Desai, T., Tunable, A., 2016. Biodegradable, thin-film polymer device as a long-acting implant delivering tenofovir alafenamide fumarate for HIV pre-exposure prophylaxis. Pharm. Res. 33 (7), 1649–1656.
Schliecker, G., Schmidt, C., Fuchs, S., Wombacher, R., Kissel, T., 2003. Hydrolytic degradation of poly (lactide-co-glycolide) films: effect of oligomers on degradation rate and crystallinity. Int. J. Pharm. 266 (1), 39–49.
Shastri, V.P., 2003. Non-degradable biocompatible polymers in medicine: past, present and future. Curr. Pharm. Biotechnol. 4 (5), 331–337.
Siegel, S.J., Winey, K.I., Gur, R.E., Lenox, R.H., Bilker, W.B., Ikeda, D., Gandhi, N., Zhang, W.-X., 2002. Surgically implantable long-term antipsychotic delivery systems for the treatment of Schizophrenia. Neuropsychopharmacology 26 (6), 817–823.
Siegel, S.J., Kahn, J.B., Metzger, K., Winey, K.I., Werner, K., Dan, N., 2006. Effect of drug type on the degradation rate of PLGA matrices. Eur. J. Pharm. Biopharm. 64 (3), 287–293.
Spreen, W., Min, S., Ford, S., Chen, S., Lou, Y., Bomar, M., St Clair, M., Piscitelli, S., Fujiwara, T., 2013. Pharmacokinetics, safety, and monotherapy antiviral activity of GSK1265744, an HIV integrase strand transfer inhibitor. HIV Clinic. Trials 14 (5), 192–203.
Spreen, W., Ford, S.L., Chen, S., Wilfret, D., Margolis, D., Gould, E., Piscitelli, S., 2014. GSK1265744 pharmacokinetics in plasma and tissue after single-dose long-acting

injectable administration in healthy subjects. J. Acquired Immune Deficien. Syndrom. (1999) 67 (5), 481–486.
Stewart, S.A., Domínguez-Robles, J., McIlorum, V.J., Mancuso, E., Lamprou, D.A., Donnelly, R.F., Larrañeta, E., 2020. Development of a biodegradable subcutaneous implant for prolonged drug delivery using 3D printing. Pharmaceutics 12 (2), 105.
Uhm, S., Pope, R., Schmidt, A., Bazella, C., Perriera, L., 2016. Home or office etonogestrel implant insertion after pregnancy: a randomized trial. Contraception 94 (5), 567–571.
Wahl, A., Swanson, M.D., Nochi, T., Olesen, R., Denton, P.W., Chateau, M., Garcia, J.V., 2012. Human breast milk and antiretrovirals dramatically reduce oral HIV-1 transmission in BLT humanized mice. PLoS Pathog. 8 (6), e1002732.
Wang, C.-K., Wang, W.-Y., Meyer, R.F., Liang, Y., Winey, K.I., Siegel, S.J., 2010. A rapid method for creating drug implants: translating laboratory-based methods into a scalable manufacturing process. J Biomed Mater Res B Appl Biomater 93 (2), 562–572.
Wang, S., Liu, R., Fu, Y., Kao, W.J., 2020. Release mechanisms and applications of drug delivery systems for extended-release. Expert Opin. Drug Deliv. 17 (9), 1289–1304.
Widmer, M.S., Gupta, P.K., Lu, L., Meszlenyi, R.K., Evans, G.R., Brandt, K., Savel, T., Gurlek, A., Patrick Jr., C.W., Mikos, A.G., 1998a. Manufacture of porous biodegradable polymer conduits by an extrusion process for guided tissue regeneration. Biomaterials 19 (21), 1945–1955.
Widmer, M.S., Gupta, P.K., Lu, L., Meszlenyi, R.K., Evans, G.R.D., Brandt, K., Savel, T., Gurlek, A., Patrick, C.W., Mikos, A.G., 1998b. Manufacture of porous biodegradable polymer conduits by an extrusion process for guided tissue regeneration. Biomaterials 19 (21), 1945–1955.
Zajc, N., Obreza, A., Bele, M., Srcic, S., 2005. Physical properties and dissolution behaviour of nifedipine/mannitol solid dispersions prepared by hot melt method. Int. J. Pharm. 291 (1–2), 51–58.
Zhou, T., Lewis, H., Foster, R.E., Schwendeman, S.P., 1998. Development of a multiple-drug delivery implant for intraocular management of proliferative vitreoretinopathy. J. Control. Release 55 (2), 281–295.